

INVESTIGATION OF BARRIER PROPERTIES OF AS CAST AND
BIAXIALLY STRETCHED PET/EVOH AND PETI/EVOH BLEND
FILMS

by

CAHİT DALGIÇDIR

Submitted to the Graduate School of Sabancı University
in partial fulfillment of the requirements for the degree of
Master of Science

Sabancı University

Summer, 2009

© Name 2008

All Rights Reserved

INVESTIGATION OF BARRIER PROPERTIES OF
PET/EVOH AND PETI/EVOH BLENDS

Cahit Dalgıçdır

MAT, Master's Thesis, 2009

Thesis Advisor: Prof. Yusuf Mencilođlu

Co-Advisor: Dr. İlhan Özen

Keywords: PET, PETI, EVOH, Permeability, Gas Barrier, Orientation

APPROVED BY

Prof. Dr. Yusuf Mencilođlu
(Thesis Advisor)

Dr. İlhan Özen
(Co-Advisor)

Asst. Prof. Melih Papila

Dr. George Wagner

Dr. Yakup Ülçer

DATE OF APPROVAL:

Abstract

In this study, poly(ethylene terephthalate)(PET)/poly(ethylene-co-vinyl alcohol)(EVOH) (95/5 w/w) and poly(ethylene terephthalate-co-isophthalate) random copolymer containing 10 wt.% isophthalic acid (PETI)/EVOH (95/5 w/w) blends have been prepared with compatibilizer types as poly(ethylene terephthalate)-co-sulfonated isophthalate (PET-co-SIPA), glycol modified poly(ethylene terephthalate) (PETG) and hydroxyl-terminated polybutadiene (HTPB) by using a co-rotating intermeshing twin screw extruder. Cast films have been stretched simultaneously and biaxially 2 and 3 times their original dimensions ($\lambda=2$, $\lambda=3$). The effects of biaxial orientation, crystallinity, morphology, and chemistry on oxygen gas permeability were analyzed by using different characterization techniques i.e. scanning electron microscopy (SEM), differential scanning calorimetry (DSC), and gas permeability analyzer.

After extrusion, the dispersed phase has a particle size of 0.4-0.8 μm without a compatibilizer. Replacing PET homopolymer with PETI has little effect on particle size of the dispersed phase (0.4-0.5 μm) without using a compatibilizer. The smallest particle size of EVOH was 0.17-0.2 μm for PET blends when employed a hydroxyl terminated polybutadiene (HTPB) and 0.15-0.25 μm (glycol modified PET, PETG) and 0.18-0.26 μm (HTPB) for PETI blends.

Oxygen gas permeability of the blend films reduces to some extent after stretching. Nonetheless, an increase in oxygen gas permeability has been observed when the results of the neat PET and PETI taken into consideration. This situation results from low degree of crystallinity of the blends. Casted and oriented PET/EVOH films show decreased water vapor permeability values when compared to that of neat PET. The lowest value has been obtained when employed HTPB as the compatibilizer. Casted films of PETI/EVOH blends have higher water vapor permeability values than that of the neat PETI. Water vapor permeability values decrease when films stretched 2 times and 3 times. Nonetheless, comparison of the results together with that of the neat PETI indicates that water vapor permeability values of the stretched films are almost the same as PETI.

Özet

Bu çalışmada Poli(etilen tereftalat)(PET)/Poli(etilen-co-vinil alkol)(EVOH) (ağırlıkça 95/5) ve %10 izofitalik asit içeren PET kopolimeri (PETI)/EVOH karışımları (ağırlıkça 95/5) değişik kompatibilizerler kullanılarak çift burgulu ekstruderde hazırlanmıştır. Dökme filmler Iwamoto marka çift eksenli gerdirme cihazında iki eksenle eşzamanlı olarak orjinal boyutlarının 2 ve 3 katına gerdirilmiştir ($\lambda:2$ ve $\lambda:3$). Taramalı elektron mikroskobu (SEM), diferansiyel taramalı kalorimetre (DSC), ve gaz geçirgenlik testleri gibi farklı karakterizasyon teknikleri kullanılarak kristallinite, morfoloji (dolambaçlı yol), ve kimyanın gaz geçirgenliği üzerindeki etkileri analiz edilmiştir.

Ekstrüzyon sonrası, kompatibilizer içermeyen numunelerdeki dispers fazın parçacık büyüklüğü 0.4 ilâ 0.8 μm arasındadır. PET homopolimeri PETI ile değiştirdiğimizde dispers fazın parçacık büyüklüğünün 0.4 - 0.5 μm civarı çıktı. PET karışımları arasında en küçük parçacık büyüklüğü 0.17 - 0.2 μm ile hidrosil sonlu polibütadiende (HTPB) görüldü. PETI karışımlarında ise, en küçük parçacık büyüklüğü 0.15 - 0.25 μm ile glikol modifiyeli PET (PETG) ve 0.18 - 0.26 μm ile HTPB'de görüldü.

Filmlerin oksijen gaz geçirgenliklerinin, filmler gerdirildikten sonra belli bir oranda düştüğü gözlemlendi. Ancak, katkısız PET ve PETI filmlerde, gerdirme sonrasında oksijen gaz geçirgenliklerin düştüğü gözlemlendi. Bu durum karışımlardaki kristallenme oranlarındaki düşüşten kaynaklanmaktadır. Dökme ve gerdirilmiş PET/EVOH filmlerin nem geçirgenlikleri, katkısız PET filmlerine oranla daha düşüktür. Nem geçirgenlik analizlerindeki en düşük değer HTPB kompatibilizer olarak kullanıldığında ortaya çıkmıştır. PETI/EVOH karışımlarının dökme filmlerinin nem geçirgenlik değerleri, katkısız PETI filmlerine oranla daha yüksek çıkmıştır. Filmler 2 veya 3 katı gerdirildiklerinde, filmlerin nem geçirgenlik değerlerinin düştüğü gözlemlenmiştir. Katkısız PETI filmlerde ise, nem geçirgenlik değerleri dökme filmler ile gerdirilmiş filmler arasında herhangi bir fark olmadığını göstermektedir.

Acknowledgements

I want to express my gratitude to my advisor Yusuf Mencelođlu for his understanding and support throughout my graduate study. I would like to gratefully acknowledge the enthusiastic supervision of İlhan Özen and his neverending patience in editing this thesis. I thank the jury members, Melih Papila, George Wagner and Yakup Ülçer for their helpful comments on the subject. I would like to acknowledge the help of Gülay Bozoklu who studied the PET/MXD6 films. I would like to thank to Mükerrerem Çakmak and his group from University of Akron for the stretching of films, Mete Karagözlü and Seda Aksel for their helps in characterization of the samples and Canan Atılğan for her help in the simulation of PET/MXD6 blends.

I would also like to express my gratitude to Funda İnceođlu who has helped me so much to come to where I am today. I am grateful to all my friends from Sabanci University: Gökhan, İbrahim, Emre, Özge, Eren, Çınar, Özlem, Burcu, Zuhale, Firuze, Özlem Z., Deniz, Elif, Burcu, Murat, Sinem, Lale, Shalima, Kerem, Vanya for being the surrogate family during the many years I stayed in Sabanci University.

Last but not least, I would like to thank my family: my parents, my brother, my grandmothers and aunt, and Enise for their endless encouragement and support.

This study was supported by TÜBİTAK

Contents

I	Introduction	1
1	Previous Work	2
2	Permeation in Polymeric Materials	3
2.1	Permeation in Polymers	3
2.1.1	Gas Permeation	5
2.1.2	Water Vapor Permeation	7
3	Barrier Polymers	8
3.1	Poly(ethylene terephthalate) (PET)	9
3.2	Ethylene-Vinyl Alcohol Copolymer (EVOH)	10
4	Parameters Affecting Barrier Properties	12
4.1	Chain Structure	12
4.2	Orientation	13
4.3	Morphology	14
5	Barrier Technologies	15
5.1	Nanocomposites	15
5.2	Multilayer Co-extrusion	15
5.3	Polymer Blending	16
II	Experimental	17
6	Materials	17
7	Sample Preparation	18
7.1	Preparation of the Blends	19
7.2	Preparation of the Films	19
7.3	Drawing	20
8	Characterization and Analysis	20
8.1	Thermal Analysis	20
8.2	Morphology	21
8.3	Oxygen Permeability	21
8.4	Water Vapor Permeability	21

III Results and Discussion	22
9 Thermal Behaviour	22
10 Crystallinity	27
11 Morphology	32
12 Oxygen Permeability	33
13 Water Vapor Permeability	42
14 Further Notes	47
IV Conclusion	48
V Future Work	49
A Mass Transfer in Polymeric Materials [1]	50
References	57

List of Figures

1	Mechanism for gas permeation [2]	4
2	Gas transmission rate, permeability, permeance relation [2]	5
3	Transmission rate test methods [3]	6
4	Gas permeation from crystalline and amorphous regions	12
5	Schematics of uniaxial and biaxial drawing	13
6	Structures achieved in polymer blending	14
7	Hydraulic clamps of the Iwamoto biaxial stretcher	20
8	DSC thermograms of the materials used	22
9	Glass transition temperatures of films	24
10	Cold crystallization temperature of films	26
11	Melting temperatures of films	28
12	Crystallinity percentages of films	29
13	Comparison of oxygen permeability values of neat PET and PETI films . .	38
14	Comparison of oxygen permeability values of cast PET and PETI blends . .	38
15	Correlation of oxygen permeability and crystallinity percentage in cast and 2 times stretched PET blends	39
16	Comparison of oxygen permeability and crystallinity percentage in 3 times stretched PET blends	40
17	Comparison of oxygen permeability values of cast and stretched PET Blends	41
18	Comparison of oxygen permeability values of cast and stretched PETI Blends	41
19	Comparison of water vapor permeability values of neat PET and PETI . .	43
20	Comparison of cast PETI and PETI Blends	43
21	Comparison of water vapor permeability values of cast and stretched PET blends	44
22	Comparison of water vapor permeability values of cast and stretched PETI blends	45
23	Correlation of water vapor permeability and crystallinity percentages in PET blends	46
24	Comparison of oxygen permeability values of all sample films	51
25	Comparison of water vapor permeability values of all sample films	52
26	Permeability and crystallinity percentages values of films	53
27	DSC thermograms of cast PET blends	54
28	DSC thermograms of cast PETI blends	54
29	DSC thermograms of 2 times stretched PET blends . . .	55
30	DSC thermograms of 2 times stretched PETI blends . .	55
31	DSC thermograms of 3 times stretched PET blends . . .	56
32	DSC thermograms of 3 times stretched PETI blends . .	56

List of Tables

1	Unit conversion for permeability [4]	7
2	Properties of PET [5]	9
3	Properties of EVOH copolymer [6]	11
4	Chemical structure of materials	18
5	Notation and percentage of blends	18
6	Glass transition temperatures of PET and PETI based cast and stretched films	23
7	Cold crystallization temperatures of cast and stretched PET and PETI blends	25
8	Melting temperatures of PET and PETI based cast and stretched films	27
9	Percent crystallinity of PET and PETI based cast and stretched films	31
10	EVOH particle size distribution of the blends	32
11	SEM images of cast PET blends	34
12	SEM images of cast PETI blends	35
13	SEM images of stretched ($\lambda:2$) PET blends	36
14	SEM images of stretched ($\lambda:2$) PETI blends	37
15	Oxygen permeability values of cast and stretched films	42
16	Water vapor permeability values of samples	47

List of Abbreviations

PET: Poly(ethylene terephthalate)

PETI / PET-co-10I: PET copolymer containing 10 % isophthalic acid

EVOH: Ethylene-vinyl alcohol copolymer with 32 mol % ethylene

N-MXD6: Poly(m-xylene adipamide)

PETG: Glycol modified poly(ethylene terephthalate)

PET-co-SIPA: Poly(ethylene terephthalate) copolymer sulfonated isophthalate

HTPB: Hydroxyl-terminated polybutadiene

PP: Polypropylene

PE: Polyethylene

PS: Polystyrene

SEM: Scanning Electron Microscope

DSC: Dynamic Scanning Calorimetry

Tg: Glass Transition Temperature

Tm: Melting Temperature

Tcc: Cold Crystallization Temperature

GTR: Gas Transmission Rate

OTR: Oxygen Transmission Rate

OP: Oxygen Permeability

WVP: Water Vapor Permeability

Part I

Introduction

The total sales of market of the packaging industry was approximately \$500 billion globally in 2008 and is expected to increase by 23 % within 5 years [7]. While packaging materials of paper, cardboard, and plastics constitute 36 % of the market, the market share of food and beverage applications of packaging market amounts to 58 % [8]. Plastics are preferred in packaging industry for their low cost, light weight and flexibility of their functionality. Most common polymers used in packaging are PP, PE, PS, and PET [9, 10, 11].

The main function of a packaging product is to protect and preserve the substance, its flavor and quality. Therefore the package should be able to provide sufficient physical and barrier protection according to the needs of contained product [12]. Glass, paper and metal have been widely used as packages but plastics have been replacing these substances at increasing rate [10]. For example, one of the current targets of research is to generalize the usage of PET in beer bottles instead of glass and metal. The recyclability and flexibility of processing of PET attracts the bottle producers towards the usage of plastics. Blending is considered to be the suitable method in order to develop, but so far there is no satisfactory blend due to cost limitation [13].

In beer packaging usually kegs, bottles and cans are used. In recent years plastic beer bottles have emerged in markets. But the plastic beer bottles lack the excellent barrier properties of aluminum cans and glass bottles. One of the disadvantages of plastic packaging in beer is transparency and high permeance to oxygen when compared to the properties of glass and aluminum [14]. With the plastics, light interferes with the fermentation process thus resulting in a decrease in flavor. Therefore, beer in plastic bottles has a very limited shelf life. The plastic bottles seen in markets have mostly green colors, although green is one of the poorer barrier colors, consumers however choose green over other better barrier colors such as red [15, 14]. Thus packaging also depends on consumer's aesthetic preference, and superior barrier qualities are not always the first choice.

The objective of this study is to investigate the barrier properties of PET/EVOH and PETI/EVOH blend films and understand the factors affecting the barrier properties of polymeric substance. Different chemicals such as PET-co-SIPA, PETG and HTPB have been added as compatibilizers to study the differences in the final properties of each blend. This study aims to contribute to the literature in the understanding of the connection of polymer properties such as polymer chemistry,

crystallinity, orientation and morphology. Blends have been prepared by extrusion and then cast as film sheets. Thermal, morphological and barrier characterization of the cast films have been performed.

1 Previous Work

In the previous work of this study, Gülay Bozoklu, Dr. İlhan Özen and Prof. Dr. Yusuf Menciloğlu analyzed the effects of poly(metaxylene adipamide) (MXD-6) incorporation into PET and PET-co-10I matrix polymers on barrier properties. PET-co-SIPA, CTPB and HTPB were used as compatibilizers and cobalt acetate as oxidation catalyst. MXD-6 was used as an oxidizable component for oxygen scavenging effect to reduce the oxygen permeability of the packaging product. N-MXD6 provides 20 times better barrier capacity than PET and its processing temperature is similar to PET; therefore N-MXD6 can be blended easily [14]. For the oxygen barrier systems, barrier capacity depends on the composition of the blend, which in this study is the 5 wt % addition of N-MXD6, and the rate of consumption for oxygen correlates with the thickness of the packaging film [16]. The results indicated that N-MXD6 had a better compatibility with PET-co-10I matrix phase, and, lowest particle sizes were achieved in both matrix polymers when PET-co-5SIPA was used as a compatibilizer [17].

After orientation, the barrier properties of 2 times ($\lambda:2$) drawn samples tended to improve whereas the 3 times ($\lambda:3$) drawn samples have shown microvoids. The higher decrease in both oxygen and water vapor permeability of the 2 times ($\lambda:2$) drawn PET samples compared to 2 times drawn ($\lambda:2$) PETI samples, was the result of increased crystallinity which was the result of the strain induced crystallization due to drawing process. Generally orientation of the samples resulted in better barrier properties in PET/N-MXD6 and PETI/N-MXD6 blend films [18].

2 Permeation in Polymeric Materials

The main functions of the package are to keep the oxygen and carbon dioxide out of the product, to contain the product environment and to prevent high water uptake and loss. Gas permeation is an important topic in polymer based packages. As permeance of polymeric packages is higher than glass and metals, for some products higher gas barrier properties are needed to achieve a proper shelf-life. Therefore there are many studies in literature regarding gas permeation in plastic films [4, 19, 20, 21, 22].

2.1 Permeation in Polymers

Metal and glass are the perfect gas barriers as the strictly ordered structure of these materials cannot allow oxygen or carbon dioxide for permeation. Therefore metal and glass have long been used as the main packaging products before polymers. The network structure of the polymers are arranged so that there are interstices between the molecular chains. Small molecules can diffuse through the paths using these interstices. These interstices constitute the free volume of the polymer. Gaseous penetrants are sorbed into and diffuse through the free volume of polymer.

$$\textit{Permeability} = \textit{Permeance} * \textit{Thickness} \quad (1)$$

$$\textit{Permeability} = \textit{Diffusivity} * \textit{Solubility} \quad (2)$$

Permeance is the amount of the penetrant molecule passing through the parallel surfaces of a barrier in a unit time. Permeability can be found by multiplying permeance with thickness of the film. So, permeability does not change with thickness whereas permeance does; therefore permeability is the intrinsic property of the material [23, 2, 24]. By using Equation 1 permeability is calculated after a permeability measurement. The permeability measurement gives the permeance values and these values are multiplied by thickness to achieve permeability. Therefore Equation 1 refers to the experimental side whereas Equation 2 refers to a theoretical basis of gas permeation in polymeric materials. According to Equation 2 permeability is the product of solubility and diffusivity. Solubility is dependent on the amount of free volume in the polymer film. It is simply the filling of the interstices in the polymer structure by the penetrant molecule. Therefore the higher the free volume, the higher the solubility. Sorption consists of condensation of the gaseous penetrant

and mixing with the polymer matrix. Condensation and mixing occur very fast and constants for most polymers are independent of chemical structure for these processes, thus sorption is not the rate-determining step in gas permeation under atmospheric pressure for most polymers like PET, PE, LDPE etc.. Considering this, most studies concentrate on tailoring the diffusivity constants of the polymer films [25, 23].

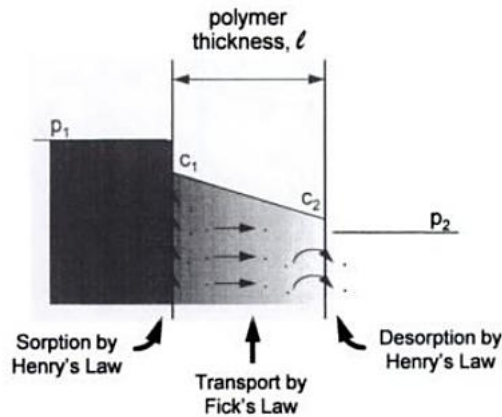


Figure 1: Mechanism for gas permeation [2]

Diffusivity depends upon the local segmental motion of the polymer chains. As the motion of these chains increases, the probability of leaving behind an interstice increases also. Diffusion occurs through these interstices, thus factors affecting molecular motion like temperature or conformational changes, also affect permeability. Diffusion of molecules includes multiple rearrangements in the local structure: the penetrant molecule finds an equilibrium position in this local structure of the material in each of the rearrangements, constituting the diffusion process. Therefore, the diffusion of molecules requires energy increasing with the size of the penetrant [2, 26]. The permeation mechanism can be seen in Figure 1, and according to this figure, in the sorption and desorption processes where the penetrant is absorbed into the matrix Henry's law is used, the transport of the penetrant molecule by diffusion is explained by Fick's law. Henry's law and Fick's law are explained in terms of mass transfer in polymeric substances in the Appendix.

To sum up, the mechanism runs like this: oxygen molecules are absorbed and mixed into the free volume in the surface of the polymer structure. Then the oxygen molecules migrate through the gaps created by the segmental motions in the amorphous section of the polymer to the opposite surface by diffusion steps. Each of these diffusion steps includes the overcome of each of the barriers requiring sufficient

energy. Finally, molecules are desorbed out of the polymer film to the ambience. The number of desorbed oxygen molecules in the final stage is the amount of oxygen molecules passing through the film gives the permeability of the film [25, 23].

$$P = \frac{Q}{tA(f/b)} \quad (3)$$

$$J = \frac{Q}{tA} \quad (4)$$

In equation 4, J represents the flux, in other words, it is the transmission rate (either gas or water vapor). Q is the amount of penetrant passing through the film, t is time and A is the unit area. In equation 3, P is permeability and b is the thickness. f represents the potential, that is the pressure difference between the opposite sides of the film. f/b then becomes the potential gradient. The correlation between these concepts is summarized in Figure 2 where WVTR is the water vapor transmission rate and Δp is the pressure difference.

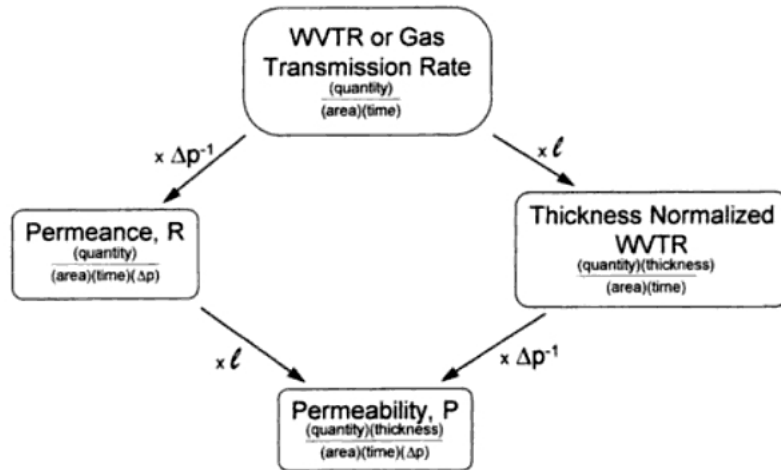


Figure 2: Gas transmission rate, permeability, permeance relation [2]

2.1.1 Gas Permeation

Gas transmission rate (GTR) and oxygen transmission rate (OTR) give the amount of gas that passes through a unit area between the opposite surfaces of a film in a unit time. Currently, there are two methods for transmission rate measurements: The equal pressure method and the differential pressure method. In the equal pressure method, nitrogen and oxygen gases at equal pressures flow from the

opposite sides of the film, oxygen flowing through the upper side and nitrogen the lower side of the polymer film. The difference of these sides are the partial pressures of oxygen; therefore oxygen molecules diffuse through the sample film to the nitrogen side, and with the help of sensors, oxygen partial pressure is detected and oxygen transmission rate can be calculated. Whereas in the differential pressure method, the sample film divides the testing area into two sections, one at a constant pressure of penetrant test gas, the other side in a vacuum. The differences in methods can be seen in Figure 3. The amount of penetrant gas passing through the film is detected by sensors and transmission rate is calculated. In this study quasi isostatic equal pressure method is used for transmission rate measurements.

$$\frac{dm_{gas}}{dt} = P \frac{A \Delta p}{l} \quad (5)$$

The left hand side of the Equation 5 represents the transmission rate of the penetrant: P is the permeability, A is the area, l is the thickness of the barrier film, and Δp is the partial pressure difference. Transmission rate is directly related to permeability of the polymer film/gas molecule complex and the thickness of the film. Both testing methods use the partial pressure parameter to determine transmission rates.

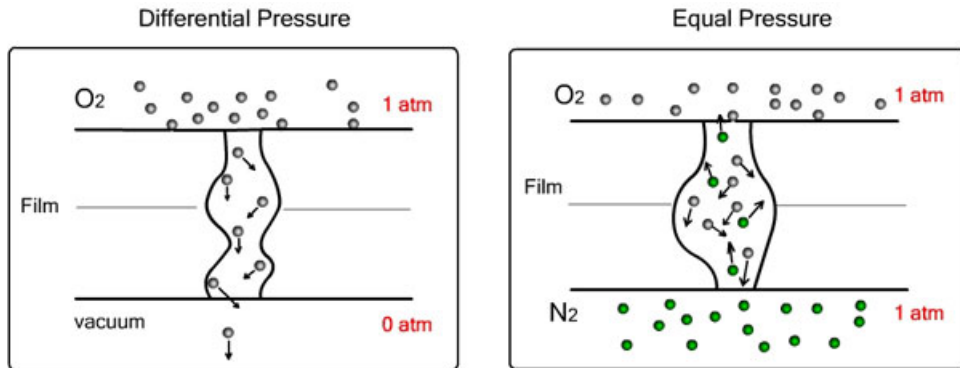


Figure 3: Transmission rate test methods [3]

Oxygen is more harmful than water for food products because it leads to lipid oxidation thus leading to permanent change in the chemistry of the substances [12]. Oxidation also interferes with the flavor of the product. Therefore for increased shelf-life it is important that gas permeation is kept at low levels. For carbonated beverages, the containment of carbon dioxide is an of great importance for the packaging bottles. Because carbon dioxide acts as an important flavor for these beverages, thus loss of carbon dioxide over the critical amount renders the product

useless. Containment of the gaseous substances within the product or the product environment is also one of the main properties of packages.

There are currently more than 20 units for measuring permeability. In this study, $ml.cm/m^2.day$ is used. Huglin and Zakaria studied listed the conversion table for these permeability units in their study, the list can be seen in Table 1 where r.p.u is defined as $10^{-10}.cm^3.cm/cm^2.s.cm Hg$ [4].

Table 1: Unit conversion for permeability [4]

Item	Miscellaneous Unit	To convert to r.p.u., multiply by:
1	(mol)/(m · s · bar)	2.99×10^{10}
2	(mol)/(m · s · atm)	2.95×10^{10}
3	(mol)/(cm · s · atm)	2.95×10^{12}
4	(mol)/(cm · s · cm Hg)	2.24×10^{14}
5	(g · mm)/(m ² · day · cm Hg)	$2.59 \times 10^4/M$
6	(g · mil)/(100 in ² · 24 hr · atm)	$1.34 \times 10^2/M$
7	(m ²)/(s)	2.99×10^{10}
8	(m ³ · m)/(m ² · s · MPa)	1.33×10^{11}
9	(m ³ · m)/(m ² · d · PPa)	1.54×10^{-3}
10	(μL · cm)/(cm ² · hr · mm Hg)	2.78×10^4
11	(μL · cm)/(cm ² · hr · kPa)	3.73×10^3
12	(cm ³ · μ)/(m ² · min · mm Hg)	16.7
13	(cm ³ · μm)/(m ² · s · kPa)	1.32×10^2
14	(cm ³ · cm)/(cm ² · d · bar)	1.54×10^3
15	(cm ³ · cm)/(cm ² · d · Pa)	1.54×10^8
16	(cm ³ · cm)/(cm ² · s · atm)	1.32×10^8
17	(cm ³ · cm)/(cm ² · s · cm Hg)	1×10^{10}
18	(cm ³ · cm)/(cm ² · s · 10 mm Hg)	1×10^{10}
19	(cm ³ · cm)/(cm ² · s · mm Hg)	1×10^{11}
20	(cm ³ · mm)/(cm ² · s · cm Hg)	1×10^9
21	(10 ⁻¹⁰ · cm ³ · cm)/(cm ² · s · cm Hg)	1.00
22	(cm ³)/(cm · s · Torr)	1×10^{11}
23	(cm ³ · mil)/(100 in ² · 24 hr · atm)	6.00×10^{-3}
24	(cm ²)/(s)	2.99×10^6
25	(ft ³ · mil)/(ft ² · min · atm)	5.09×10^5
26	(in ³ · mil)/(100 in ² · 24 hr · atm)	9.82×10^{-2}
27	(cm)/(s)	$2.99 \times 10^6 \times b$
28	(mol)/(cm ² · min · atm)	$4.91 \times 10^{10} \times b$
29	centibarrer	1.00×10^{-2}

2.1.2 Water Vapor Permeation

Water binds to the food products by hydrogen bonding. Water gain or loss of the product changes its flavor and its crispiness. Water gain, after a certain level, may also lead to increase an in bacterial activity, which will putrefy the product and make the substance unedible. The higher the water uptake is, the quicker the food product will putrefy, rendering the packaging film low-grade. Therefore, it is

important that the package should not let water vapor into or out of the packaged environment.

The absorption of water into the polymer leads to plasticization in the film as a result of decrease in cohesive energy density i.e. inter- and intra- molecular attraction between the hydrogen bonds on the chains, as the water molecules constitute space between and thus obstruct such molecular interactions between the polymer chains. The obstruction of these interactions result in increase in free volume and more interstices are formed between the molecular chains. Increase in free volume is the same as the increase of the possible number of paths of the penetrant molecule. Thus, plasticization of polymer films results in decrease in their mechanical and barrier properties [27, 23].

$$a_w = \frac{P}{P_0} = \frac{\%ERH}{100} \quad (6)$$

%ERH: Equal Relative Humidity of the substance

P : vapor pressure of water in the substance

P_0 : vapor pressure of neat water

Water activity in Equation 6 gives information as to whether the substance will gain water or lose water when exposed to air. Relative humidity is the ratio of the humidity of the substance divided by the maximum humidity that can be achieved. If the relative humidity of the substance is high when exposed the substance will lose water; but if relative humidity is low, then the substance will gain water according to their water activities. The main purpose of the packaging product is to diminish the process of water uptake and loss [25, 12, 26].

3 Barrier Polymers

Volatile compounds e.g. alcohols, esters, phenols are important for the flavor of beer. The binding of these volatile substances to the packaging product decreases the oxygen barrier properties of the packaging material, thereby degrading the flavor of the compound. The binding process increases with the amount of amorphous structure in the package [28]. Thus crystalline polymers i.e. PET and EVOH are affected less by this absorption process, whereas amorphous polymers e.g. LDPE suffer the most from this phenomena.

3.1 Poly(ethylene terephthalate) (PET)

Poly(ethylene terephthalate) is a condensation polymer. It is synthesized using para-xylene to form terephthalic acid (or dimethyl terephthalate) and ethylene to form ethylene glycol. Then the product chemicals go through a condensation mechanism to produce water or methanol according to usage of either terephthalic acid or dimethyl terephthalate respectively [5, 29]. Table 2 shows some of the properties of PET.

PET has a high crystallization, very good gas barrier properties, excellent mechanical properties, chemical resistance, and excellent transparency. The biaxially oriented PET is widely used as carbonated beverage bottles [28, 30]. One disadvantage of PET is its low melt strength due to short chain branches inherent in its structure and narrow molecular weight distribution, thereby, making PET unsuitable for extrusion blow molding. The low melt strength problem can be overcome by copolymerization of PET to achieve a better melt strength to be able to process with extrusion blow molding [6, 29, 31]. As an example glycol modified PET (PETG) can be given, which is produced by copolymerization of cyclohexane dimethanol with ethylene glycol and terephthalic acid. The melt strength of PETG is better than PET, so that it can be processed by extrusion blow molding. PETG also has high clarity and toughness; therefore, it is used mainly as bottles and in packaging of food products and also as medical devices [6, 5, 32].

Table 2: Properties of PET[5]

Properties of PET	
T_g	73-80 $^{\circ}C$
T_m	245-265 $^{\circ}C$
Density	1.29 - 1.40 $\frac{g}{cm^3}$
Tensile strength	48.2-72.3 MPa
Maximum Elongation	30-3000 %
WVTR	390-510 $\left(\frac{g \cdot \mu m}{m^2 \cdot day}\right)$ @ 37.8 $^{\circ}C$, 90 % RH
O_2 Permeability	1.2-2.4 x 10 ³ $\left(\frac{cm^3 \cdot \mu m}{m^2 \cdot d \cdot atm}\right)$
CO_2 Permeability	5.9-9.8 x 10 ³ $\left(\frac{cm^3 \cdot \mu m}{m^2 \cdot d \cdot atm}\right)$

In packaging industry, PET is one the most often used polymers, thanks to its clarity and barrier properties compared to the other packaging polymers e.g. PS, HDPE and PP. Aside from beverages, due to its recyclability, PET is also used in food packaging applications. Recent efforts have been made to use PET in beer bottles. However there are disadvantages related to the usage of PET in beer packaging

industry. The first one is the transparency of PET; the second, the lower barrier properties compared to those of other widely used beer bottles: aluminum and glass. The transparency can be eliminated by using colored PET bottles which are opaque to certain wavelengths that are most effective in preventing flavor spoilage. The barrier properties can be increased by several methods, multilayer or monolayer, blending with barrier resins or oxygen scavengers. There are also other obstacles that arise during the processing of beer. For example, beer is pasteurized above 60°C, but the mechanical strength of PET bottles fails at these temperatures. To overcome this problem, PET is heat-set during blow-molding, increasing thickness and thus strength to tolerate the pasteurization process. The monolayer structure has been more accepted in the literature to be a better route for beer packaging, thanks to the relative simplicity and flexibility of the method. However there are currently few inexpensive methods for application [14, 13].

3.2 Ethylene-Vinyl Alcohol Copolymer (EVOH)

EVOH is melt processable and thermally stable, strong, tough, and also it possesses excellent gas barrier properties due to the high crystallinity achieved as a result of the ability of hydroxyl and hydrogen groups residing in the same crystal lattice sites as well as resistance to chemicals such as solvents and hydrocarbons [17, 33]. EVOH is obtained by hydrolyzing the copolymerization product of ethylene and vinyl acetate. Vinyl alcohol employs polarity to EVOH by the hydroxyl groups in the backbone, increasing the intermolecular forces, whereas the ethylene section sustains the mobility of the chains. The amount of ethylene and vinyl alcohol may be varied to achieve a more compatible structure for the target penetrating compound. Mostly 32 % mol and 44 % mol of ethylene in EVOH is used in packaging applications. As the percentage of ethylene decreases, the barrier property of the polymer increases at dry media because of the higher hydroxyl group content forming strong hydrogen bonds between the chains. However the higher vinyl alcohol content increases moisture sensitivity and decreases the processability of the polymer [6, 27, 33].

The main disadvantage of EVOH can be seen when the penetrant molecules have high polarity. The barrier property of EVOH to polar substances is very low due to the hydroxyl groups coming from the vinyl part of EVOH on the polymer backbone. The projection of this drawback, especially in the packaging of food products, occurs at humid media. At a high amount of humidity EVOH fails to barricade water vapor. As EVOH is hydrophilic, its solubility in water is higher than its solubility in other mainstream packaging polymers. Therefore, water vapor disrupts the hydro-

gen bonding between the polymer chains and decreases the barrier properties of the polymer [16, 6, 27, 34, 35]. Cava et. al found in their study that at low relative humidity, i.e. at 23%, gas barrier properties of EVOH increase due to water molecules binding with the hydroxyl groups to some extent and blocking the free volume of the polymer matrix. Thus, the clustering of the water molecules decreases the gas permeation flux [34]. Because of this moisture problem, EVOH is mainly used as an inner layer to packaging products. For example, it is coextruded and sandwiched between films that have good moisture barrier properties, e.g. polyolefins. In these techniques an adhesive is used to bind the polar EVOH and nonpolar polyolefin, or, alternatively, a desiccant may also be used in the tie layer [6, 9, 27, 36].

EVOH is not very compatible with other polymers like PP, PET, PE or PS; therefore, several compatibilizers, preferably ionomers or polymers with maleic anhydride or acrylic acid groups, are used for blending processes or tie-layers are used to bind the EVOH with outer polymers in multilayer films [33, 37, 38]. The reason behind this behaviour is clearly explained by Coleman et al. in their study as: "... EVOH copolymers are self-associated, while the inter-association of the hydroxyl groups of EVOH with the carbonyl groups of the complementary polymers is comparatively weak" [39].

The miscibility of EVOH is also affected by the ethylene content; the higher the ethylene content, the lower the miscibility of EVOH with other polymers is [40]. EVOH has been used as a packaging product for many applications including juices, cheese, solvents, chemicals etc. Its growing usage has been extended to fuel tanks and protective clothing and because of its superior barrier properties, studies concerning EVOH copolymer blends with polyamides are increasing [28, 41]. Some of the physical and thermal properties of EVOH constituting 32% ethylene are listed in Table 3.

Table 3: Properties of EVOH copolymer[6]

Property	EVOH 32% Ethylene
Density $\frac{g}{cm^3}$	1.19
Tensile Strength, MPa	88
Tear Strength, $\frac{N}{mm}$	154
T_m , $^{\circ}C$	181
T_g , $^{\circ}C$	70
Heat Seal Temperature, $^{\circ}C$	179-238
Oxygen Permeability, $\left(\frac{cm^3*\mu m}{m^2*day*atm}\right)$	
0% RH	4
65% RH	13
WVTR, $\frac{g*\mu m}{m^2*day}$ (@38 $^{\circ}C$ 90% RH)	2500

4 Parameters Affecting Barrier Properties

4.1 Chain Structure

The lowest energy state in a polymer occurs in its crystal form. This state corresponds to the lowest Gibbs free energy of the system. For crystallinity to be achieved, the atoms in the polymer chains should be regularly packed. Therefore polymers with similar structure as PE and PVC crystallize easily due to their symmetrical, linear arrangement. Whereas polymers that have bulky substituents such as aromatic rings as in PET, crystallization occurs more slowly [42, 6]. In the case of PET, the reason for the high amount of crystallinity is the 1,4 *para*-linkage. In an *iso* substituent where the *meta*-linkage occurs in 1,3 positions i.e. poly(ethylene isophthalate) PEI, the polymer is amorphous, i.e. the arrangement of the molecules are obstructed due to the bulky substituents. This behaviour can be tracked when PET is copolymerized with PEI; as the amount of PEI increases crystallinity decreases and after the addition of 20 % of PEI, the resulting polymer becomes amorphous [43].

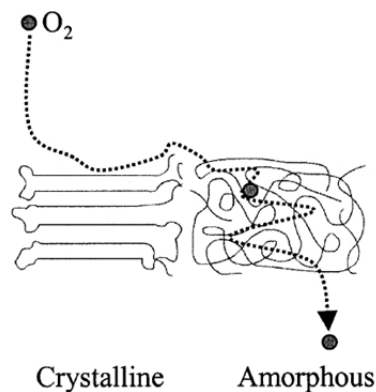


Figure 4: Gas permeation from crystalline and amorphous regions

The barrier properties of the packaging products are controlled by the crystalline structure and the degree of crystallinity of the PET matrix [44]. The degree of crystallinity is simply the fraction of crystallinity in the polymer, assuming the polymer is made up of two regions which have the same properties as their ideal states: amorphous and crystalline. The mass or volume fraction of the crystalline region provides the degree of crystallinity. There are many methods for characterizing degree of crystallinity of a polymer. In this study DSC measurements are used; the percent crystallinity is achieved by the Equation 7. Because the permeation of small

molecules such as oxygen and carbon dioxide is much less in crystalline regions than the amorphous regions, the permeability is therefore directly related to the amount of crystallinity in the structure [45].

$$Crystallinity\% = 100 * \frac{PeakArea(melt) - PeakArea(coldcrystallization)}{Enthalpy(Melt, 100\%Crystallinity)} \quad (7)$$

4.2 Orientation

The orientation of PET by drawing results in the transformation of *gauche* conformers to *trans* conformers; therefore, the *trans* segments are aligned in the direction of extension [19, 46]. Moreover, *gauche* conformers do not show any orientation due to drawing, these experimental findings as a result of FT-IR studies of oriented PET films, demonstrate that the improved barrier properties of PET are the results of these oriented *trans* conformers [47].

Above glass transition temperature polymer is drawn either uniaxially or biaxially to achieve orientation, as can be seen in Figure 5. Uniaxial drawing is done by stretching the polymer in one axis, whereas in biaxial drawing, the polymer is drawn in two axes. When the polymer is stretched, the molecular chains in the polymer elongate in the direction of the stretch.

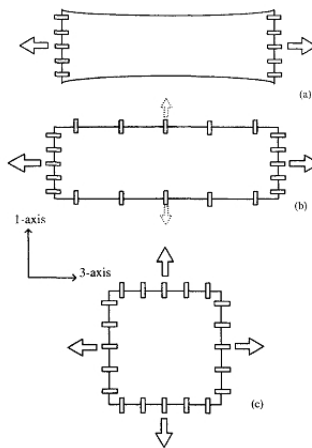


Figure 5: Schematics of uniaxial and biaxial drawing

During orientation, an ordered structure is seen which can be called as a mesophase. This mesophase is a result of the *trans* chain segments in the PET structure [48]. When the number of these *trans* segments are significantly increased, the nucleation

of crystals occurs and a network is formed which leads to strain hardening. Subsequently, strain-induced crystallization takes place [30, 49, 50]. The alignment of chains reduces the percentage of the amorphous phase and thus decreases the free volume. The decrease of free volume leads to a more dense structure, impeding the diffusion of small molecules, thus decreasing permeability [18].

Orientation, aligns the chains in the direction of drawing, increases crystallinity and increases the density of the polymer by reducing the free volume resulting in an increase in both strength of the material in the direction of drawing and barrier properties. However as the drawing factor increases, there is a risk that the film will include microtears which will decrease mechanical and barrier properties of the film if the polymer film has non-uniform thickness distribution [46].

4.3 Morphology

Although both the composition and the barrier properties of each of the components play a role in the barrier properties of the final structure, the final morphology should be taken into account [37]. The morphology of the dispersed phase plays an important role in the barrier properties of the film. A spherical morphology is obtained by blending. The spherical particles in the particulate system in Figure 6, inhibit the diffusion of small molecules through the polymer film. By drawing, on the other hand, lamellar morphology of the dispersed phase can be achieved. The lamellar morphology has better barrier properties achieved by increasing the pathway of the diffusing penetrant molecules. The lamellas are arranged so that a tortuous pathway is created for the small molecules to diffuse through [51, 52].

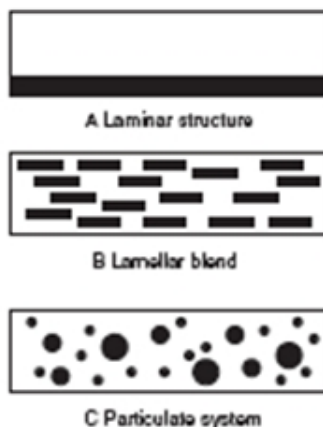


Figure 6: Structures achieved in polymer blending

5 Barrier Technologies

The gas permeation levels of polymers is higher than their packaging counterparts glass and metals. Therefore, to ameliorate the barrier properties of the polymer films, several methods have been invented in the past 60 years. Multilayer co-extrusion, blending, nanocomposites and thin coatings all serve to decrease the oxygen and carbon dioxide permeance of the polymer films for packaging applications.

5.1 Nanocomposites

Inorganic materials e.g. clay, are dispersed in the polymer matrix. Dispersion of the filler material is the key factor in this method. To achieve a uniform distribution of the filler material in the polymer matrix, either a compatibilizer can be used or the inorganic material can be treated to increase the distance between clay layers. The increased distance between the clay layers increases the amount of polymeric substance to diffuse between the layers and achieve an intercalated or exfoliated structure. The introduction of inorganic materials improves mechanical, thermal and barrier properties [53, 41]

5.2 Multilayer Co-extrusion

Multilayer coating is an appealing method in both rigid and flexible packaging in which a high barrier layer such as EVOH or MXD6 is sandwiched between inexpensive water vapor resistant plastics e.g. polypropylene or poly(ethylene terephthalate). The number of layers can be increased for different purposes. These layers are co-extruded and usually bonded with the help of proper adhesives used as tie-layers. The co-extrusion process requires multiple dies for each of the layers. For example, in multilayer PET bottles, a blend of liquid crystal polymers (LCP) and MXD6 is used. The usage of chemically suitable adhesives and multiple dies makes the process complex and more expensive than nanocomposites or blending for industrial applications. Despite the required complexity and high cost of the method, the method of multilayer casting is used for nearly 70 % of the barrier PET bottles and continue to grow. Because the higher equipment costs are leveled out by excellent target properties, which cannot be achieved by either nanocomposites or blending. One of the main drawbacks of multilayer extrusion technique is that the recyclability is limited due to the use of adhesives, as separating the adhered polymer layers is

hard [37, 51, 14, 13].

5.3 Polymer Blending

Polymer blending is a method of producing new polymers by merging superior qualities of each of the blended polymers to improve properties or develop new properties. Blending is also applied to achieve easier processable polymers, or even reduce material costs. It is a faster and less expensive method than synthesizing new polymers [54, 55, 35, 32]. There has been an increase in the usage of blending for achieving improved barrier properties in PET bottles and films in recent years [56].

The compatibility of polymers is an important factor for blending and requires strong interaction between the polymers. When polymers are not compatible, compatibilizers are used to decrease the degree phase separation. Compatibilizers generally do not change the miscibility region in the phase diagram. They are more like interfacial agent molecules that increase the degree of compatibility [57]. Achieving a compatible blend depends on the morphology; therefore, parameters affecting morphology like interfacial tension and viscosity ratio should also be taken into account for compatibility [58]. If the polymers are incompatible and no compatibilizer is used while blending, polymers are phase-separated; therefore, the target qualities cannot be achieved and the properties start to deteriorate. The blend can be characterized by DSC for melting curves to check the compatibility of the polymers. If the polymers are not compatible, two melting peaks or a broadened melting peak will be seen [59].

Compatible blends have better mechanical properties resulting from a fine dispersion of the polymers and a strongly bonded interface. Polymer compatibility is different than miscibility for example two compatible polymers may not be miscible in each other; that is, the polymers form a phase separated structure but the phase separation in the structure may be acceptable for polymer processing applications; therefore, the polymers are said to be compatible. Polymers are miscible when the Gibbs free energy of mixing is negative. Therefore, the miscibility term is an exact term, that is, it possesses an exact definition. Whereas compatibility is a term, used to define the subject at hand. That is, the compatibility of the polymers differs according to target properties. The Gibbs free energy of the polymers may be positive, but when the blend might exhibit the target qualities, then the polymers are said to be compatible. Thus, every immiscible polymers are not automatically incompatible [60].

Part II

Experimental

6 Materials

Two different PET based matrix polymers were used in this study. Matrix polymers were obtained from Artenius UK: Melinar B60 (CSD grade PET, IV: 0,82 dl/g) was used for the Poly(ethylene terephthalate) matrix and OptraH (IV: 0,82 dl/g) consisting 90 wt% terephthalic acid and 10 wt% isophthalic acid was used for the PETI matrix. EVAL SP-434, Ethylene vinyl alcohol copolymer (EVOH) was used as the dispersed phase and is obtained from EVAL, Europe N. V. which includes 32% mol. of ethylene. PET-co-5SIPA, PETG and HTPB were used as compatibilizers. PET-co-5SIPA copolymer which consists of 5% sodium sulfonated isophthalate was provided by Artenius UK. HTPB, hydroxyl-terminated polybutadiene (Krasol, LBH-P, 2000), was provided from Sartomer Company Inc. Glycol-modified PET, PETG, was obtained from Artenius UK. The molecular structures of some of the chemicals used in this study can be found in Table 4.

Table 4: Chemical structure of materials

Materials	Molecular Structure
PET	
PETI	
EVOH	
PET-co-SIPA	
PETG	
HTPB	

7 Sample Preparation

Table 5 shows the ingredients, the weight percent of the substances and the corresponding notation of the sample films.

Table 5: Notation and percentage of blends

Blend	Notation	wt. % (wt. % of compatibilizer)
PET/EVOH	EPV100	95/5
PET/EVOH (PET-co-5SIPA)	EPV101	95/5 (0.47)
PET/EVOH (PETG)	EPV102	95/5 (1)
PET/EVOH (HTPB)	EPV103	95/5 (1)
PETI/EVOH	EOV100	95/5
PETI/EVOH (PET-co-5SIPA)	EOV101	95/5 (0.47)
PETI/EVOH (PETG)	EOV102	95/5 (1)
PETI/EVOH (HTPB)	EOV103	95/5 (1)

7.1 Preparation of the Blends

Moisture content also has to be considered before processing the polymer. For example, if the polymer is PET, at even moderate amount of moisture content, there is a risk of hydrolytic degradation. Therefore to avoid degradation, PET is dried before extrusion, moisture content is lowered under 0,005 % [6]. Since PET suffers from hydrolysis at high temperatures, PET and PETI were dried at 160⁰C for 6 hours before processing [6]. PETG and PET-co-SIPA have been dried at 60-65⁰C for 3 hours. Dried granules were then purged with gaseous nitrogen in metal drums. 95/5 wt. % PET/EVOH and PETI/EVOH blends with or without a compatibilizer, were prepared by Leistritz Micro 27-GL 44D twin screw extruder (L/D ratio is 44, screw diameter is 27 mm). 100 rpm was used as screw speed and the throughput was 4.5 kg/h. Barrel temperatures have been determined as 265⁰C. The processing temperature is lower than normal processing temperature of PET, however, this temperature was chosen to avoid degradation of EVOH.

In the cast film extrusion technique, films are extruded by either single or twin screw extruders, pushed through a slit-die, cooled by chill rolls and wound by a winder. The thickness of the film can be defined by adjusting the speed of the rollers [61]. To avoid degradation of polymers, process temperature should be carefully chosen. The process temperature should be between the melting and degradation temperatures of the polymer and can be adjusted within this range to achieve the intended properties in the final polymer.

7.2 Preparation of the Films

Prior to cast film preparation, the blends were dried at 120⁰C overnight. Scientific brand Single Screw Extruder Type LE25-30/CV with Scientific brand Laboratory Cast Film and Sheet Attachment Type LCR-300 from Labtech Engineering, Thailand was used for production of cast films (L/D: 25). Both PET and PETI matrix films were prepared at 300⁰C, and chill roll was set at 65⁰C. The screw speed was set between 100-160 rpm.

7.3 Drawing

The drawing of the films was done using Iwamoto Biaxial Stretcher at the Polymer Engineering Division of the University of Akron. The films were cut by 13x13 cm, and these samples were clamped by hydraulic clamps as shown in 7. Prior to drawing, samples were kept at 90⁰C for 15 minutes to avoid any uneven heat distribution during the drawing process which might lead to uneven stretching and therefore voids. Drawing was performed at 90⁰C at a rate of 1mm/sec and the samples were stretched 2 and 3 times their original lengths.

At higher drawing temperatures, the amount of force matrix phase applies to the dispersed phase decreases, therefore, the probability of achieving the elliptical dispersed phase is lowered. At lower drawing temperatures, the molecular orientation of the polymer chains in matrix polymer is low, therefore, it is highly probable that microtears and microvoids are formed. Therefore, the temperature was chosen by taking into consideration of these factors.

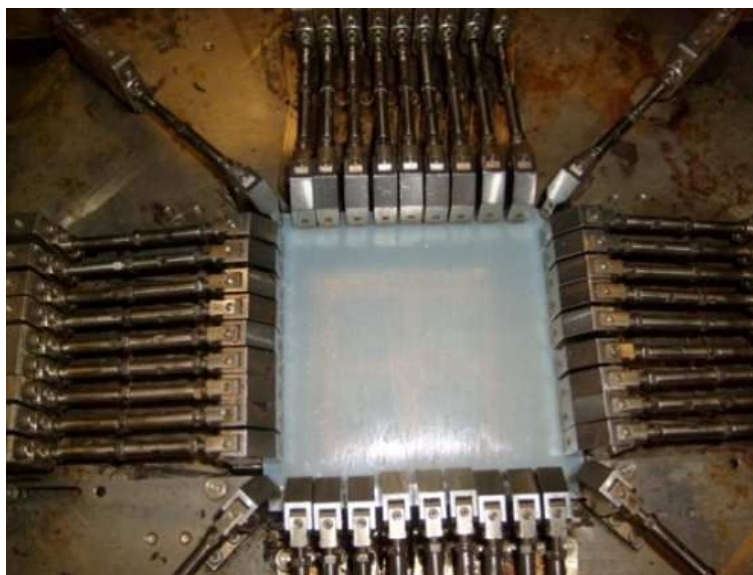


Figure 7: Hydraulic clamps of the Iwamoto biaxial stretcher

8 Characterization and Analysis

8.1 Thermal Analysis

Netsch DSC 204 was used for thermal analysis DSC measurements. The samples were heated from 20⁰C to 300⁰C by a heating rate of 5 K/min and kept for 5 minutes

isothermally, then cooled to 20⁰C with a cooling rate of 40 K/min, and again kept for 5 minutes isothermally and as a last step, heated to 300⁰C with 5 K/min. The data from the first heating rate is used for crystallinity percentage calculations.

8.2 Morphology

The film samples were dipped into liquid nitrogen and subsequently cryofractured. Then the cryofractured films were coated with carbon using Emitech K950X sputter coater to avoid charge build-up, and finally analyzed by scanning electron microscope, Leo G34-Supra 35VP with an accelerating voltage of 2 kV.

8.3 Oxygen Permeability

The oxygen permeability measurements were performed according to equal pressure method, by using Labthink TOY-C2 film-package oxygen permeability tester (designed in accordance with ASTM D3985, ASTM F1307 and ASTM F1927). The measurements were done at 25⁰C and 0 % relative humidity. Results were acquired as $\mu\text{m.ml/m}^2.\text{day}$. and then converted to $\text{ml.cm/m}^2.\text{day}$.

8.4 Water Vapor Permeability

Water vapor permeability measurements were done according to gravimetric cup method by using Labthink TSY-T3 water vapor permeability tester (designed in accordance with ASTM E96 and ASTM D1653). The measurements were performed at 38⁰C with 90 % relative humidity. The results are expressed in $\text{g.cm/m}^2.\text{day}$.

Part III

Results and Discussion

9 Thermal Behaviour

The DSC thermograms of neat PET, neat PETI, EVOH, PET-co-SIPA, PETG, and HTPB can be seen in Figure 8. EVOH has a melting point at 180⁰C, neat PET at 252⁰C, neat PETI at 241⁰C and PET-co-SIPA at 247⁰C. Cold crystallization temperature of PET is at 141⁰C, PETI at 170⁰C and PET-co-SIPA at 171⁰C. Glass transition temperature of PET is at 80⁰C, PETI at 81⁰C, PET-co-SIPA at 83⁰C and PETG is at 80⁰C . HTPB is liquid at room temperature therefore it does not have a melting temperature.

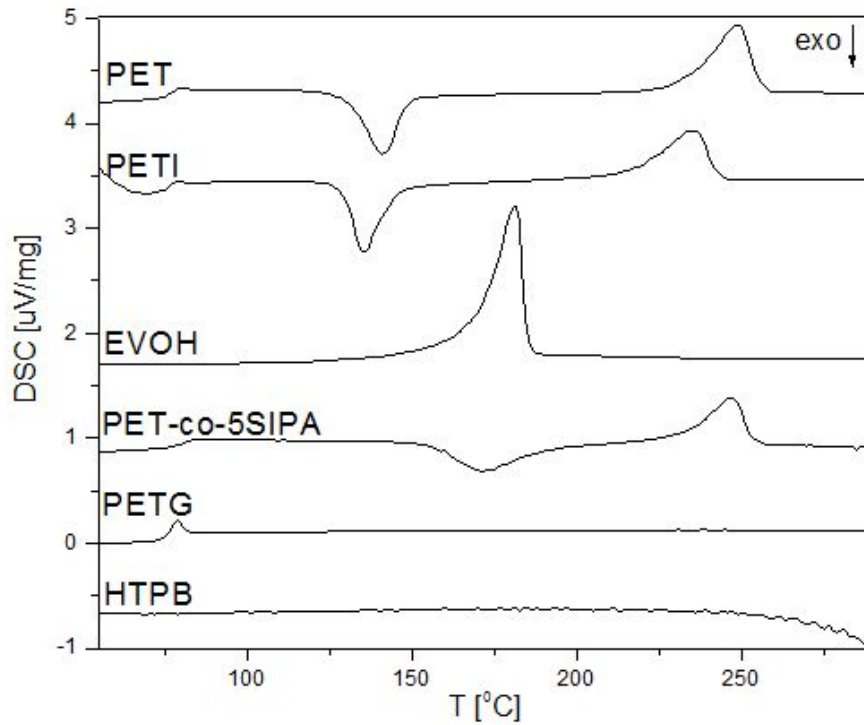


Figure 8: DSC thermograms of the materials used

Dynamic scanning calorimetry analyses indicate that 2 times stretching ($\lambda:2$) lowers the glass transition temperature however 3 times stretching ($\lambda:3$) increases it. Neat PET and neat PETI are the exceptions: in neat PET there is a linear increase,

whereas in neat PETI the Tg values in 2 times stretched ($\lambda:2$) and 3 times stretched ($\lambda:3$) are close and higher than that of the cast film. The introduction of EVOH into PET and PETI lowered the glass transition temperatures of the films except for the neat cast PETI film where an increase is encountered. The use of PET-co-SIPA as compatibilizer (EOV101) yields lower Tg values than those of the blends without compatibilizer and containing PETG (EOV102) and HTPB (EOV103).

Table 6: Glass transition temperatures of PET and PETI based cast and stretched films

Sample	Tg ($^{\circ}\text{C}$)		
	Cast Film	$\lambda:2$	$\lambda:3$
neat PET	74.6	78.7	80.3
EPV100	73.5	67.9	75.1
EPV101	71.1	73.1	72.2
EPV102	73.6	70.2	73.4
EPV103	72.7	68.1	73.3
neat PETI	68.9	77.4	76.5
EOV100	71.1	66	73
EOV101	67	64.5	72.1
EOV102	71.5	66.3	73.2
EOV103	72.7	65.8	73.9

Cold crystallization temperature (T_{cc}) of the neat PET film is 121.5°C . Stretching reduces the cold crystallization temperature of the neat PET (117°C for $\lambda:2$ and 99.4°C for $\lambda:3$). The PET/EVOH blends containing no compatibilizer (EPV100), PETG (EPV102), and HTPB (EPV103) show nearly the same behavior (cast EPV100: 121.5°C , stretched EPV100: 116°C ($\lambda:2$), and 103.5°C ($\lambda:3$); cast EPV102: 121.2°C , stretched EPV102: 121.8°C ($\lambda:2$), and 113.1°C ($\lambda:3$); cast EPV103: 119.9°C , stretched EPV103: 118.7°C ($\lambda:2$), and 107.8°C ($\lambda:3$)). Nonetheless, T_{cc} values have hardly been affected with stretching when added PET-co-SIPA (cast EPV101: 115.9°C , stretched EPV100: 117.7°C ($\lambda:2$), and 115.4°C ($\lambda:3$)). Except for the EPV101, comparison of the cast neat PET with the cast PET blends delivers no appreciable differences in terms of T_{cc} . Addition of EVOH and/or PETG and/or HTPB does not affect the cold crystallization temperature of the neat PET.

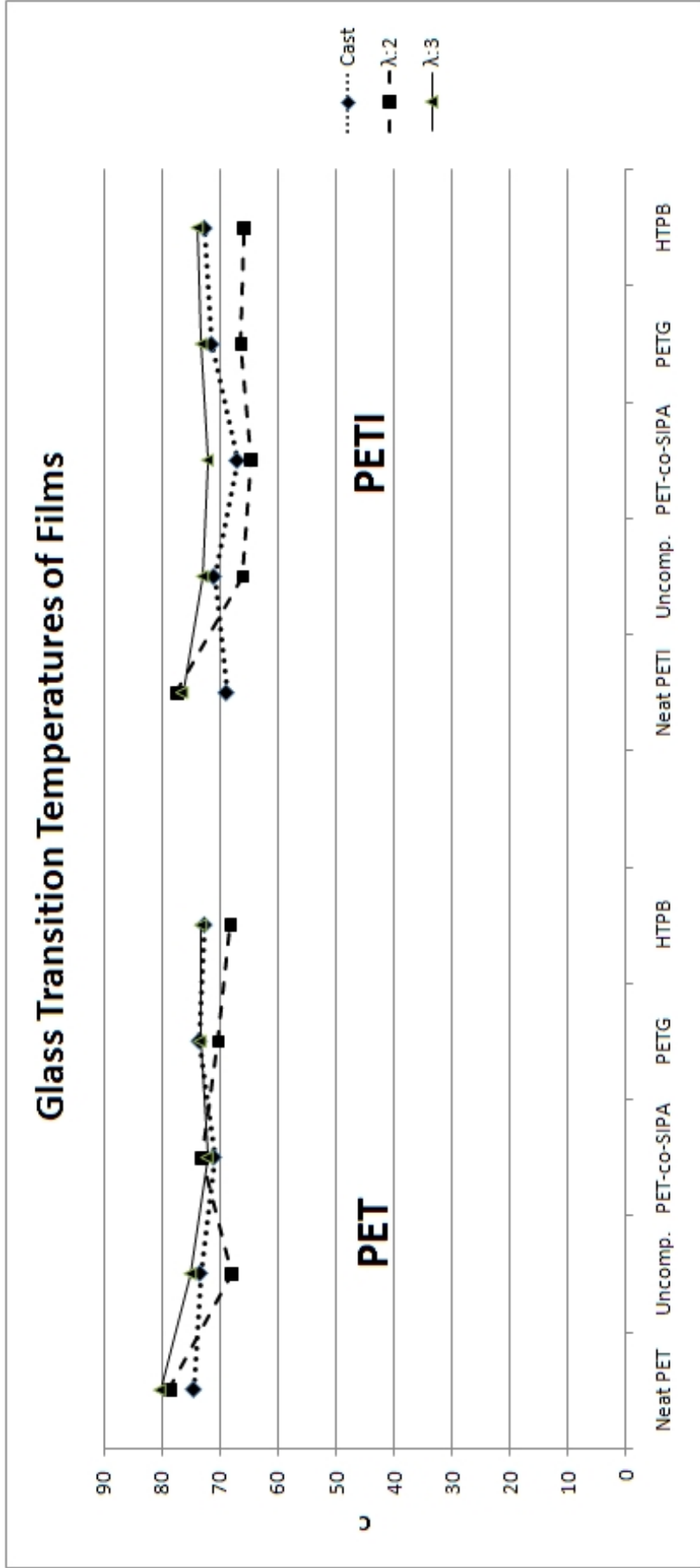


Figure 9: Glass transition temperatures of films

Table 7: Cold crystallization temperatures of cast and stretched PET and PETI blends

Sample	T _{cc} (C)		
	Cast Film	λ :2	λ :3
Neat PET	121.5	117	99.4
EPV100	121.5	116	103.5
EPV101	115.9	117.7	115.4
EPV102	121.2	121.8	113.1
EPV103	119.9	118.7	107.8
Neat PETI	125.6	119	101.2
EOV100	126.7	125.8	115
EOV101	121.4	121.8	121.3
EOV102	130.7	129.1	126.7
EOV103	124.8	117.1	122.4

PETI and its blends have the same behavior. The neat PETI show a decreased T_{cc} with stretching (neat PETI: 125.6⁰C (cast), 119⁰C (λ :2), 101.2⁰C (λ :3)). T_{cc} values of the PETI blends decrease only to a small extent with stretching. And especially in PETI blend containing PET-co-SIPA (EOV101) there has been even no observable decrease in T_{cc} (EOV101:121.4⁰C (cast), 121.8⁰C (λ :2), 121.3⁰C (λ :3)).

The drawing leads to the decrease of T_{cc} and the reduction in the area of the T_{cc} peak as the oriented amorphous chains crystallize at lower temperatures due to reduction of their entropy. Both reduction in the area of T_{cc} and a decrease in T_{cc} have been observed for the stretched PET blends. On the other hand, T_{cc} values of the stretched PETI blends (λ :2 and λ :3) remain nearly constant which points out that only amorphous chain orientation is developed perhaps due to substantial relaxation following deformation.

Table 8 shows that melting temperatures of PET/EVOH samples are between 250–252⁰C. As neat PET has a melting temperature at 252⁰C, and, EVOH at 180⁰C, it can be clearly seen from the DSC thermograms that the addition of EVOH does not change the melting temperature. Moreover, the EVOH melting peak cannot be seen in the DSC thermograms, this is due to the low amount of EVOH (5 wt.%). However in the PETI/EVOH samples, the difference is a little higher. The neat cast PETI film has a melting temperature at 241⁰C, but the cast sample with PETG (EOV102) has a melting temperature at 231.7⁰C. The PETI/EVOH blend without a compatibilizer (EOV100) and the cast PETI/EVOH film with the compatibilizer PETG, have lower glass transition temperatures compared to neat PETI film (where PETI: 68.9⁰C, EOV100: 71.1⁰C, EOV102: 71.5⁰C). The blend cast films that have

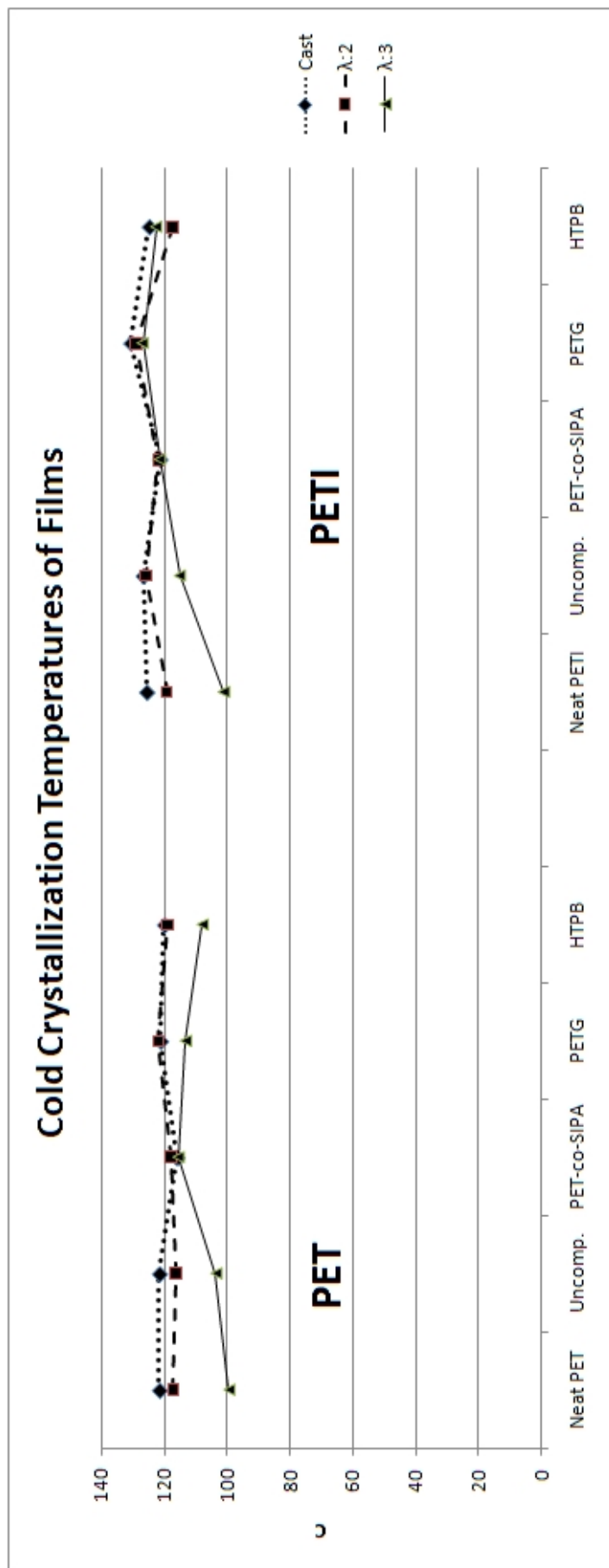


Figure 10: Cold crystallization temperature of films

PET-co-SIPA and HTPB as compatibilizers have higher melting temperatures than their counterparts (where EO101: 242.6°C, EO103: 242.5°C). It is seen that the melting temperatures of the stretched films do not have large differences with the melting temperature of the neat films.

Table 8: Melting temperatures of PET and PETI based cast and stretched films

Sample	Tm (C)		
	Cast Film	$\lambda:2$	$\lambda:3$
Neat PET	252.5	250.5	252
EPV100	251.4	250.4	250.5
EPV101	252	250.2	251.6
EPV102	251	250.3	250.2
EPV103	250	250.5	250.1
Neat PETI	241.1	240.3	238.4
EOV100	235.1	235.1	235.7
EOV101	242.6	244.5	243.9
EOV102	231.7	231.7	233.1
EOV103	242.5	239.5	240.4

10 Crystallinity

The degree of crystallinity gives the ratio of the crystal regions in the polymer versus the amorphous regions. According to the Equation 8 melting peak area and the cold crystallization is divided by the 100% crystallized PET which is 140 J/g by default; the result gives us the percentage of crystallinity in the samples. Cold crystallization peak area is subtracted from melting peak area, which is afterwards divided by the melting enthalpy of 100 % crystallized PET.

$$Crystallinity\% = 100 * \frac{PeakArea(melt) - PeakArea(coldcrystallization)}{Enthalpy(Melt, 100\%Crystallinity)} \quad (8)$$

The drawing of the films induces molecular movement which triggers orientation of the chains, thus resulting in an induction of crystallization. Therefore, an increase in crystallization by drawing is expected which eventually decreases the oxygen permeability of the films since crystalline regions in the matrix block the passage of oxygen.

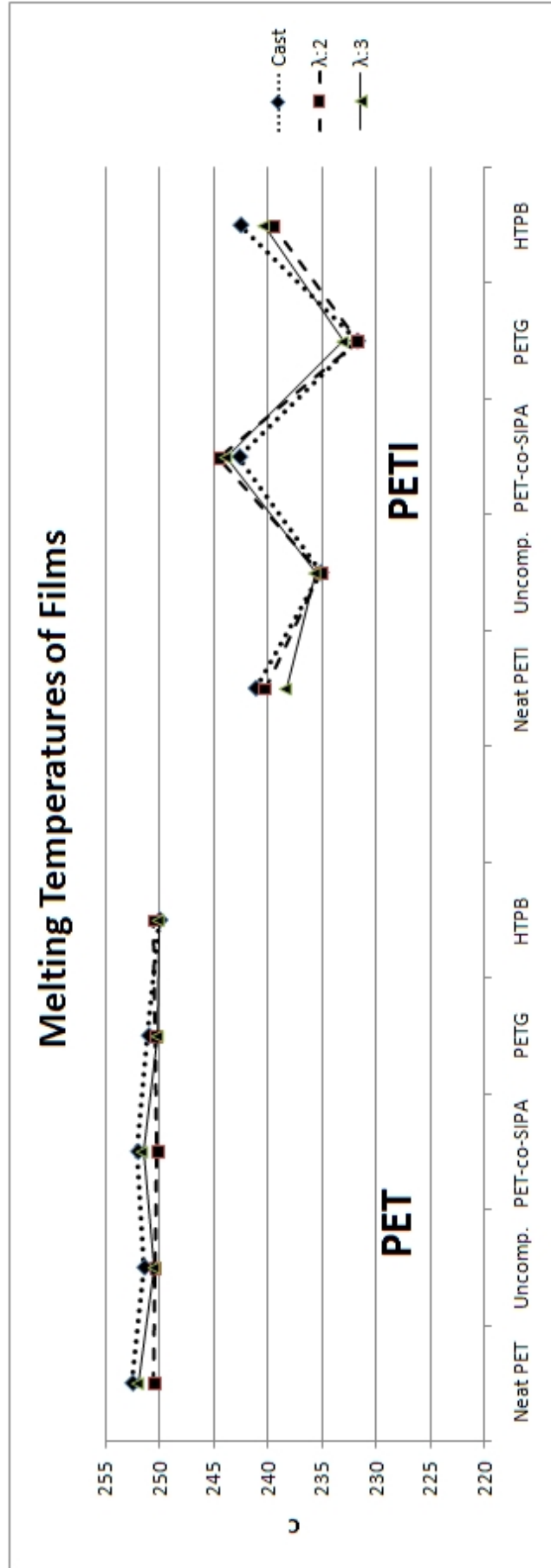


Figure 11: Melting temperatures of films

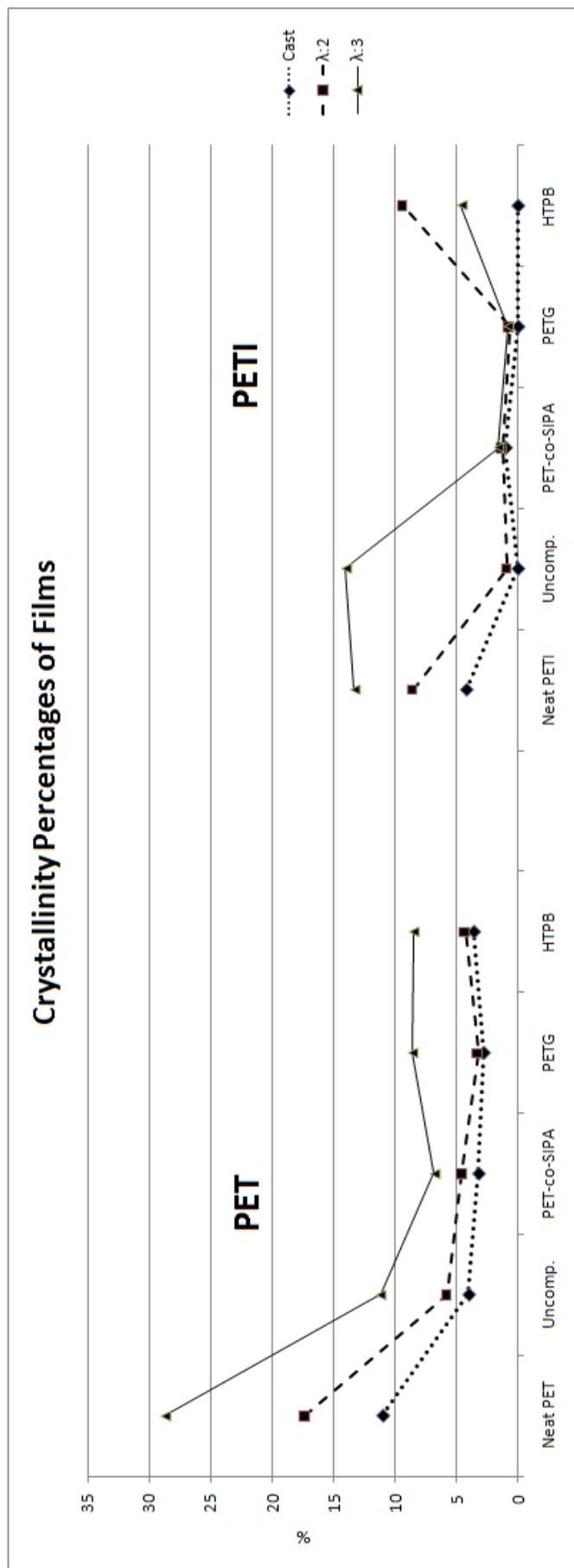


Figure 12: Crystallinity percentages of films

Table 9 reveals that stretching increases the degree of crystallinity which has been observed in the neat PET & PETI appreciably (neat PET: 11 %; stretched PET: 17.4 % ($\lambda:2$), 28.7 % ($\lambda:3$); neat PETI: 4.2 %; stretched PETI: 8.6 % ($\lambda:2$), 13.3 % ($\lambda:3$)). Addition of EVOH and the compatibilizers (PET-co-SIPA, PETG, and HTPB) decreases the degree of crystallinity when the unoriented blends are considered (PET/EVOH blend without compatibilizer EPV100: 4%, PET-co-SIPA containing EPV101: 3.2%, PETG containing EPV102: 2.8%, and HTPB containing EPV103: 3.6%). Stretching increases the degree of crystallinity in PET blends as well (neat PET: 17.4 % ($\lambda:2$), 28.7 % ($\lambda:3$); blend without the compatibilizer, EPV100: 5.8 % ($\lambda:2$), 11.2 % ($\lambda:3$); PET-co-SIPA blend, EPV101: 4.6 % ($\lambda:2$), 6.8 % ($\lambda:3$); PETG blend, EPV102: 3.3 % ($\lambda:2$), 8.6 % ($\lambda:3$); HTPB blend, EPV103: 4.3 % ($\lambda:2$), 8.5 % ($\lambda:3$)).

Degree of crystallinity of the unoriented neat PETI film increases from 4.2 % to 8.6 % for 2 times stretching and to 13.3 % for 3 times stretching. Addition of EVOH and/or the compatibilizers lowers the degrees of crystallinity of all PETI blends substantially (cast - neat PETI: 4.2 %, blend without the compatibilizer EO100: 0 %, PET-co-SIPA blend EO101: 1 %, PETG blend EO102: 0 %, HTPB blend EO103: 0 %). Moreover, stretching does not help recover the degree of crystallinity (EO100: 0.9 % ($\lambda:2$), 14 % ($\lambda:3$); EO101: 1.3 % ($\lambda:2$), 1.6 % ($\lambda:3$); EO102: 0.7 % ($\lambda:2$), 0.8 % ($\lambda:3$); EO103: 9.4 % ($\lambda:2$), 4.6 % ($\lambda:3$)).

The low amount of crystallization in EVOH blend samples can be attributed to the self-association of EVOH: as EVOH only crystallizes with itself, the low amount of EVOH (5 wt.%) reduces the intermolecular hydrogen bonds with the hydroxyl groups of EVOH and thus decreases the degree of crystallization in the EVOH dispersed phase. Besides, incorporation of EVOH into PET and PETI disrupts their structures and prevents chain alignment and thus leading to overall decrease in crystallinity in the blend samples.

High degree of crystallinity providing more crystalline parts which are impermeable to oxygen and less amorphous parts which are the only pathway for oxygen permeation leads to enhanced oxygen barrier properties in PET blends. *Meta* linkages and the *kink* structure in PETI prevent chains from crystallization which results in lower degrees of crystallinity in comparison to those of the PET blends leading to worse oxygen gas permeability. According to DSC analyses, the structure of PETI is almost totally disrupted by showing itself with crystallinity values being nearly 0%. This result is anticipated to be the result of the meta-linkage of the isophthalate, hindering the regular arrangement of the chains. Addition of EVOH and/or the compatibilizers has a detrimental effect on the degree of crystallinity when considered the results of the neat PETI. These results are in accordance with the cold

crystallization temperatures of the PET/EVOH and the PETI/EVOH blends which are closely related to the orientation of the molecules and thus crystallinity. T_{cc} values of the PET/EVOH blends are shifted to lower temperatures after stretching but the oriented PET/EVOH blends have higher cold crystallization temperatures than those of the oriented neat PET films which result in lowering the degree of crystallinity. On the other hand, T_{cc} values of the PETI/EVOH blends hardly changed.

Incorporation of EVOH into PET and PETI disrupts their structures and prevents chain alignment and thus decreases the degree of crystallinity. According to DSC analyses, the structure of PETI is almost totally disrupted by showing itself with crystallinity values being nearly 0 %. This result is anticipated to be the result of the *meta*-linkage of the isophthalate, hindering the regular arrangement of the chains.

The blends with PET matrix polymer have higher crystallinity percentages than PETI based blends. Moreover, the percentage increase in crystallinity of the PETI blends is lower than in PET blends. The decrease in percentage of crystallinity in PETI blends was expected due to the bulky substituent of the *meta*-linkage of the isophthalate hindering the regular arrangement of the chains.

Table 9: Percent crystallinity of PET and PETI based cast and stretched films

Sample	Crystallinity (%)		
	Cast Film	$\lambda:2$	$\lambda:3$
neat PET	11	17.4	28.7
EPV100	4	5.8	11.2
EPV101	3.2	4.6	6.8
EPV102	2.8	3.3	8.6
EPV103	3.6	4.3	8.5
neat PETI	4.2	8.6	13.3
EOV100	0	0.9	14
EOV101	1	1.3	1.6
EOV102	0	0.7	0.8
EOV103	0	9.4	4.6

The low amount of crystallization in EVOH blend samples can be attributed to the self-association of EVOH: as EVOH only crystallizes with itself, the low amount of EVOH (5% wt.) reduces the intermolecular hydrogen bonds with the hydroxyl groups of EVOH and thus decreases the degree of crystallization in the EVOH dispersed phase, leading to overall decrease in crystallinity in blend samples [40].

11 Morphology

Particle size distribution of the dispersed phase can be seen in Table 10. The corresponding SEM images of the PET blend films are shown in Table 11, and those of the PETI blend films in Table 12. Using PET-co-5SIPA as compatibilizer reduced the particle size of PET/EVOH blends (EPV101) from 0.4 - 0.8 μm to 0.25 - 0.35 μm . Employing PETG as compatibilizer (EPV102) reduced the particle size of the dispersed phase to 0.12 - 0.3 μm and HTPB (EPV103) reduced the particle sizes to 0.17 - 0.20 μm . PETI blends show approximately the same results (EOV100: 0.4-0.5 μm , EOV101: 0.22-0.5 μm , EOV102: 0.15-0.25 μm , EOV103: 0.18-0.26 μm). Considering all these blends, the best compatibilizer seems to be HTPB; the second, PETG; and the last, PET-co-5SIPA. All of the compatibilizers used reduced the particle size. The higher compatibility of HTPB stems from the attraction of its functional groups to hydroxyl groups of EVOH resulting in a better compatibility.

Table 13 and Table 14 include the SEM images of 2 times stretched ($\lambda:2$) PET and PETI blends, respectively. The images reveal that the dispersed phase, EVOH, is deformed. The deformation is partial in samples with 2 times stretched ($\lambda:2$) PET-co-SIPA and HTPB in both PET and PETI blends (EPV101, EPV103 and EOV101 and EOV103), i.e. the sample films exhibit both undeformed and deformed EVOH particles throughout the film. The deformation creates a lamellar structure which results in a tortuous pathway for penetrant molecules. The largest deformation is seen in the HTPB containing PET/EVOH blend (EPV103).

The SEM images of the 3 times stretched ($\lambda:3$) PET/EVOH and PETI/EVOH blends could not be obtained. Cryofracturing of the samples was not possible because of the decreased thickness and increased flexibility. Etching of the samples with nitric acid led to disintegration of the PET and PETI matrix polymers. Etching of the samples with DMSO for 20 seconds in 150⁰C led to rapid melting of the samples. Therefore, suitable samples for SEM imaging were not able to be acquired.

Table 10: EVOH particle size distribution of the blends

Notation	Particle Size (μm)
EPV100	0.4 - 0.8
EPV101	0.25 - 0.35
EPV102	0.12 - 0.3
EPV103	0.17 - 0.20
EOV100	0.4 - 0.5
EOV101	0.22 - 0.5
EOV102	0.15 - 0.25
EOV103	0.18 - 0.26

12 Oxygen Permeability

The oxygen permeability (OP) results of the both the unoriented and stretched films can be seen in Table 15. The OP value of the unoriented neat PET film reduces from 0.388 ml.cm/ m^2 .day to 0.325 (λ :2) and further down to 0.245 (λ :3). Addition of EVOH to the cast films without employing compatibilizer increases the OP (cast EPV100: 0.400), furthermore, incorporation of the compatibilizer increases the OP values, except the HTPB blend (EPV103) (PET-co-SIPA containing EPV101: 0.421, PETG containing EPV102 0.415 and HTPB containing EPV103 0.396). 2 times stretching (λ :2) leads to a reduction in OP values of uncompatibilized and HTPB compatibilized blends (EPV100: 0.341, EPV103: 0.341). An increase in OP values of the blends with PET-co-SIPA and PETG as compatibilizers has been observed (EPV101: 0.452, EPV102: 0.472). However, 3 times stretching (λ :3) improves the oxygen barrier property of the compatibilized blends (EPV101: 0.254, EPV102: 0.385, EPV103: 0.225). The OP value of 3 times stretched sample of uncompatibilized blend is lower than its cast film and higher than the 2 times stretched uncompatibilized film (EPV100: 0.375). The lowest OP value has been attained in 3 times stretched HTPB containing blend (EPV103: 0.225 (λ :3)).

Table 11: SEM images of cast PET blends

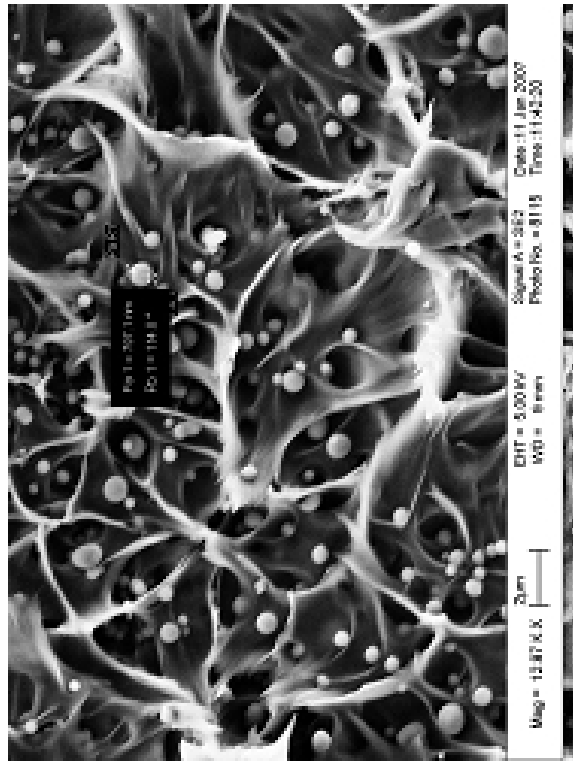
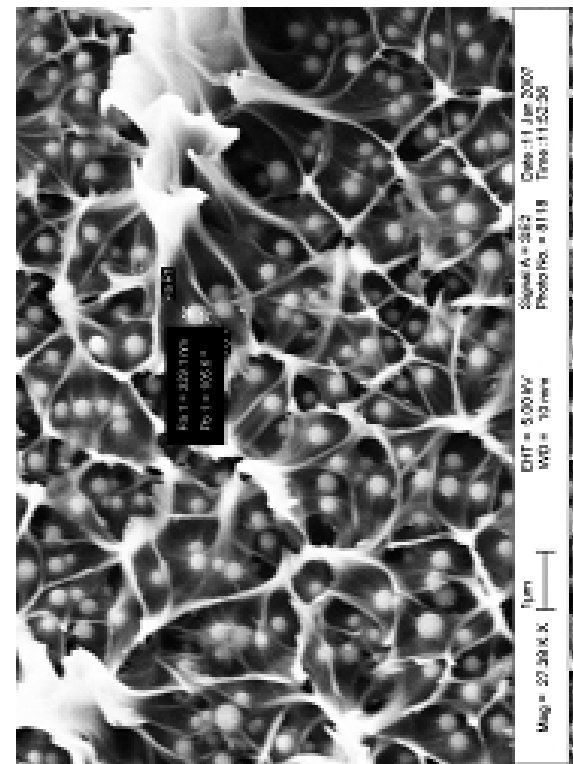
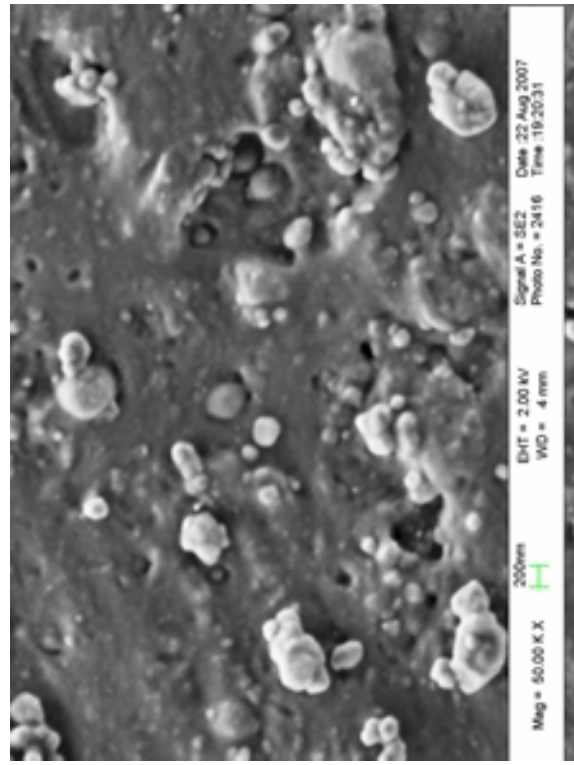
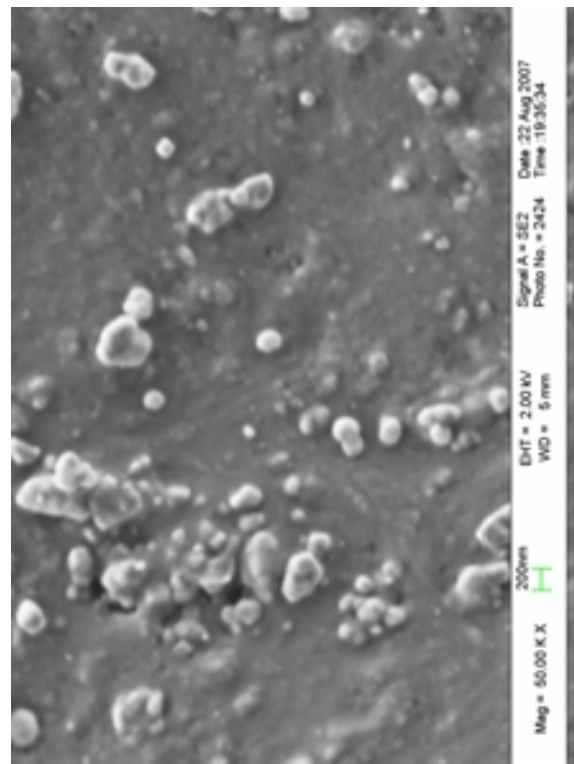
 <p>(a) EPV100</p>	 <p>(b) EPV101</p>
 <p>(c) EPV102</p>	 <p>(d) EPV103</p>

Table 12: SEM images of cast PETI blends

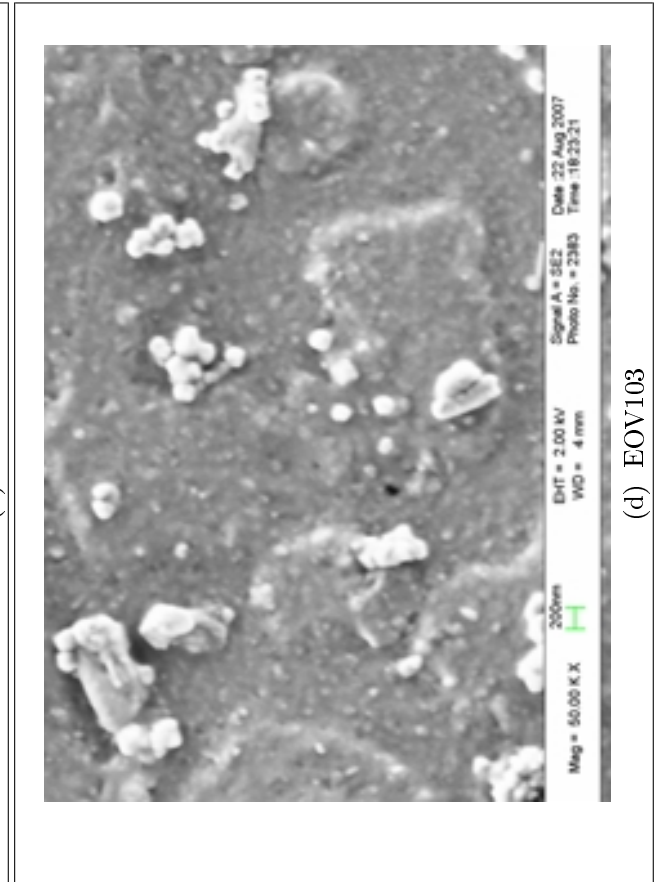
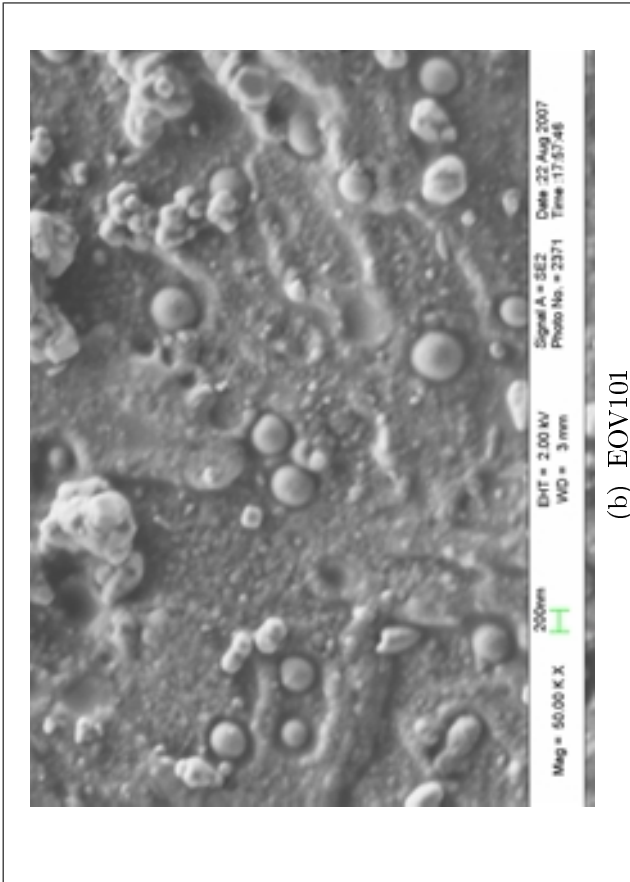
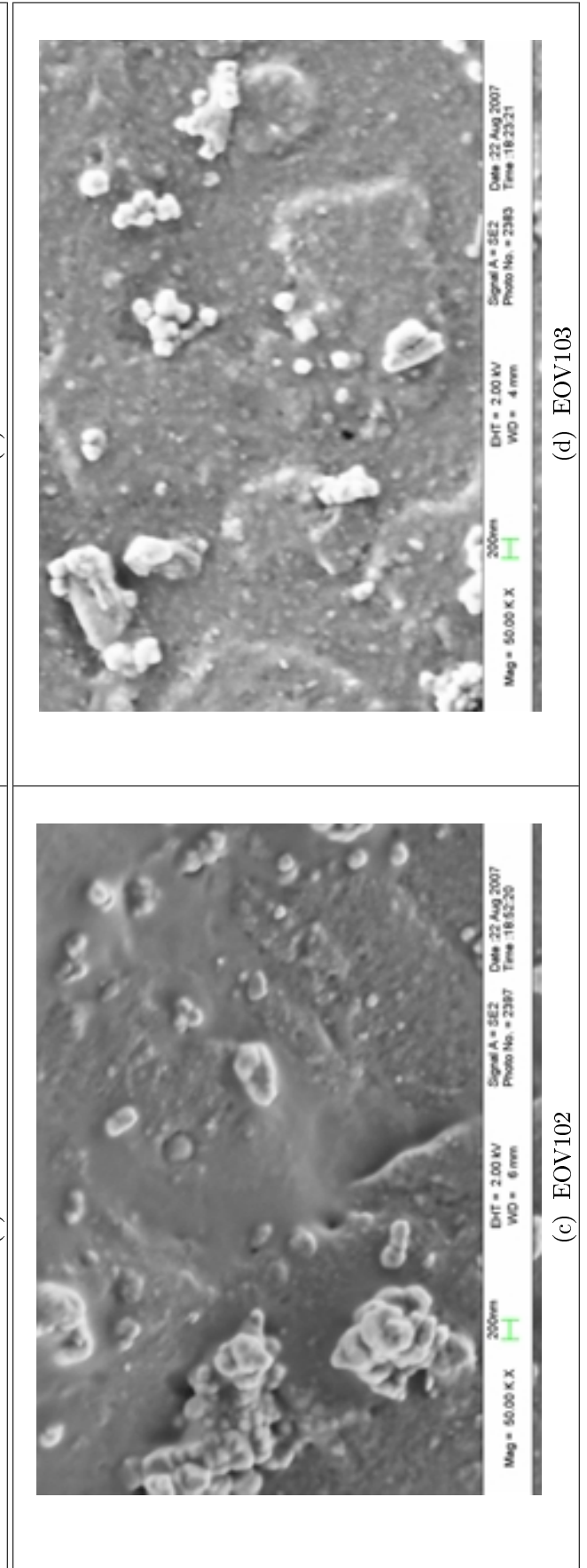
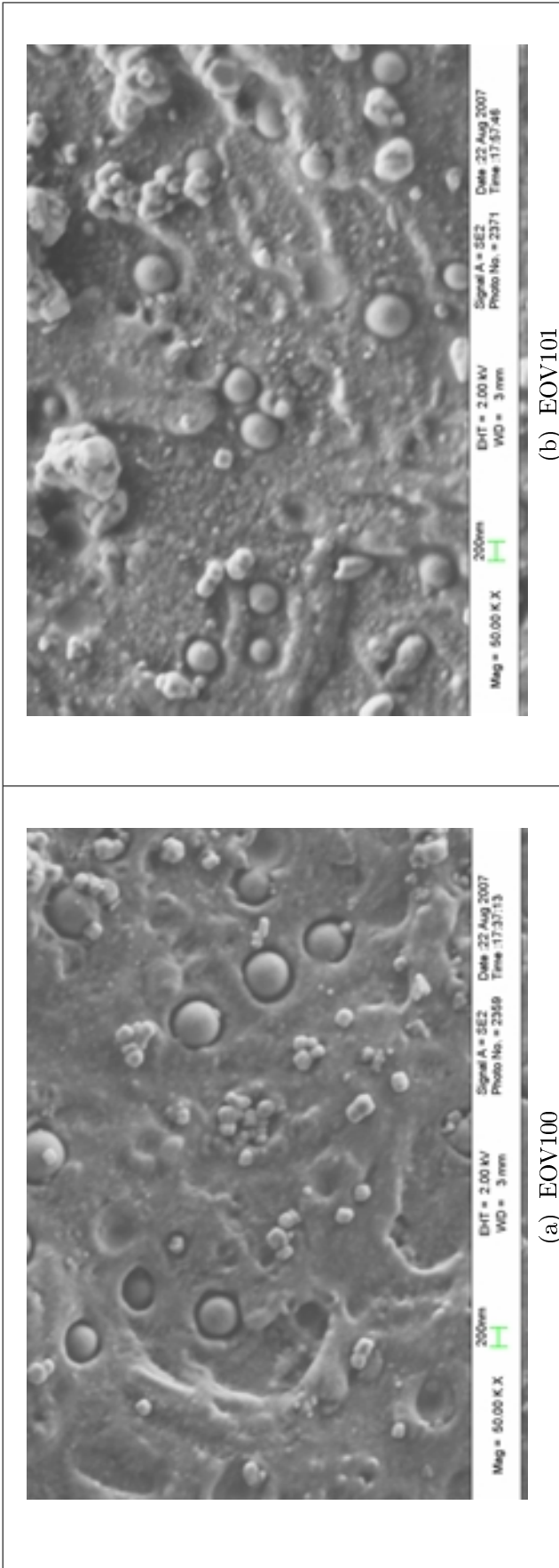


Table 13: SEM images of stretched ($\lambda:2$) PET blends

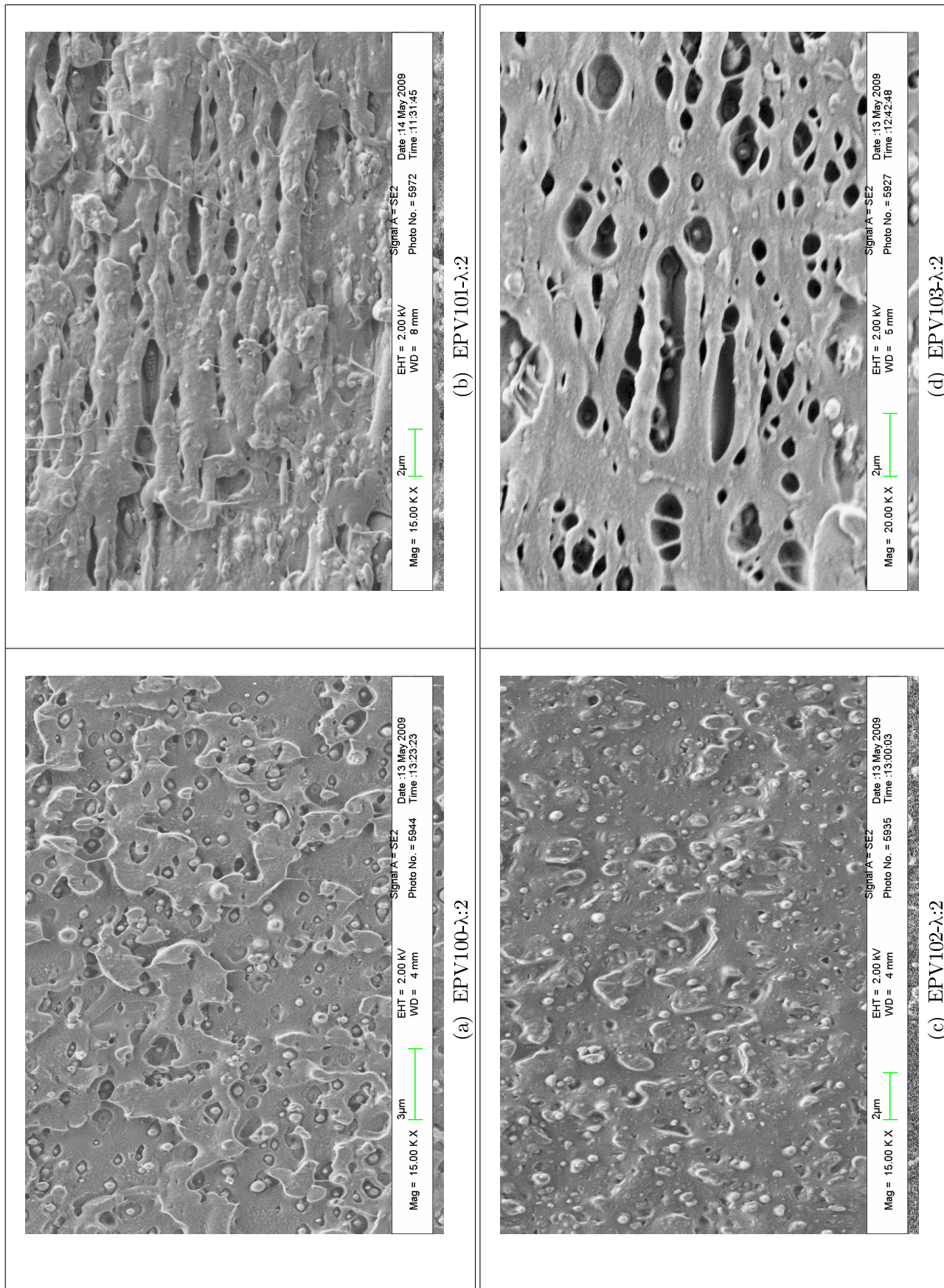
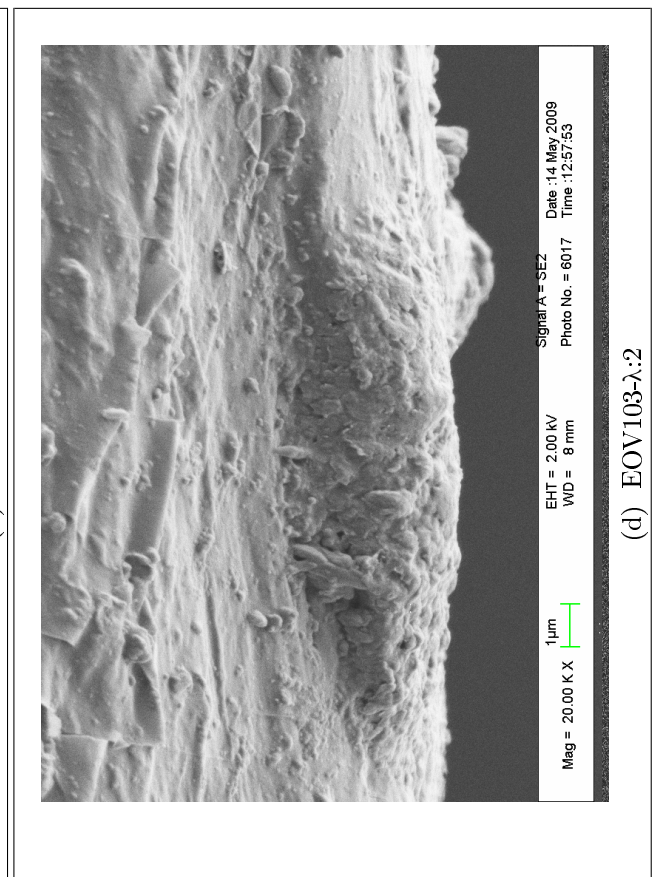
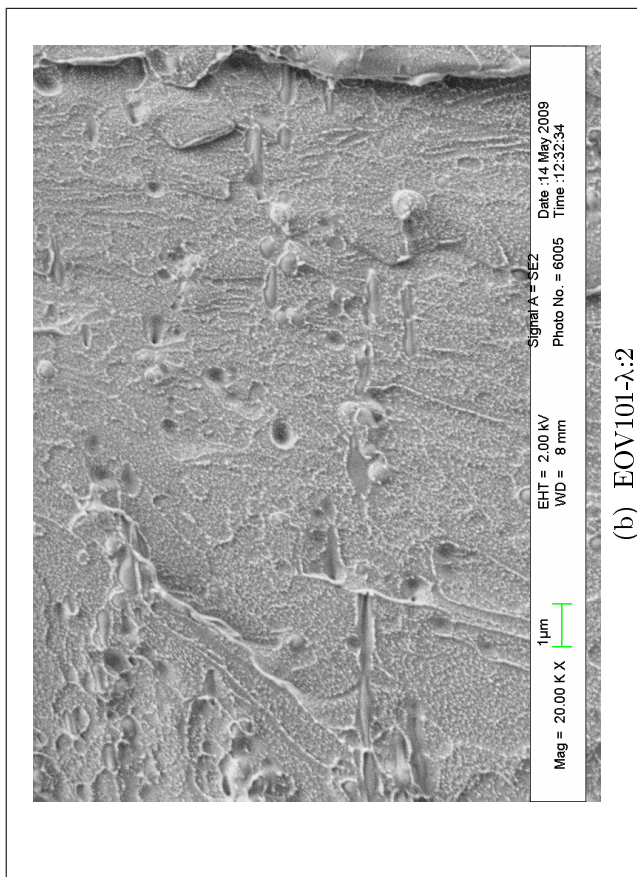
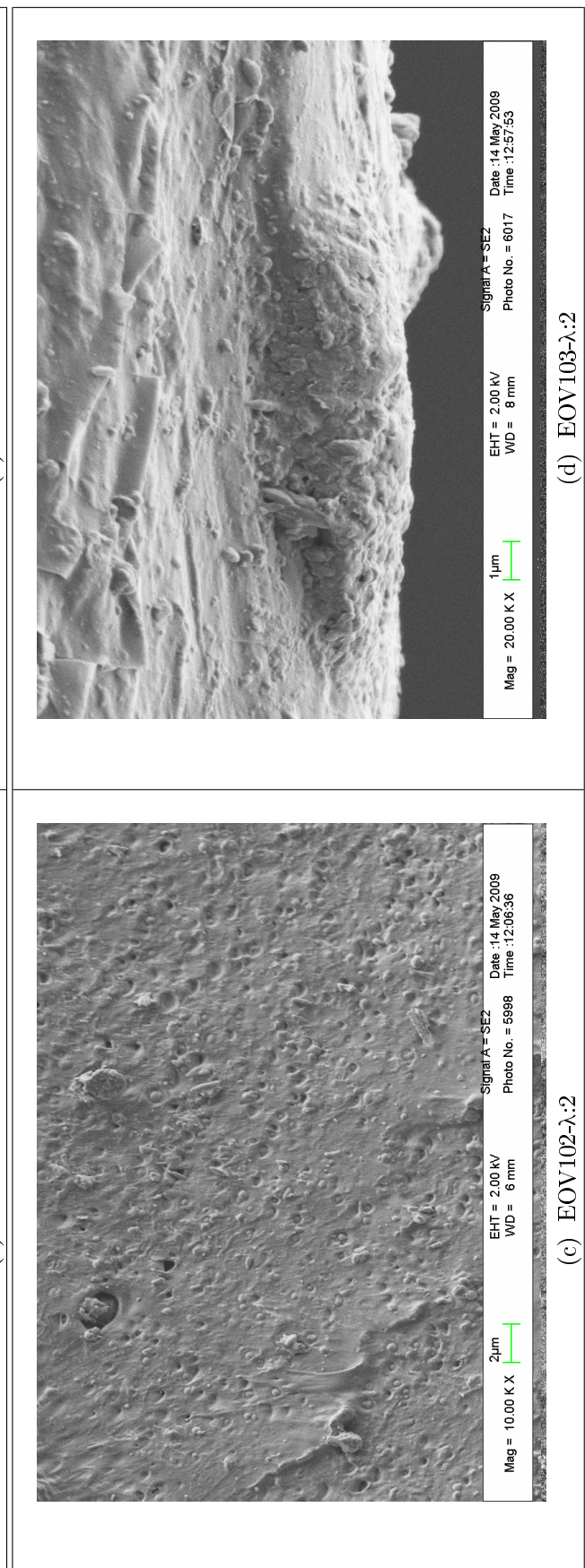
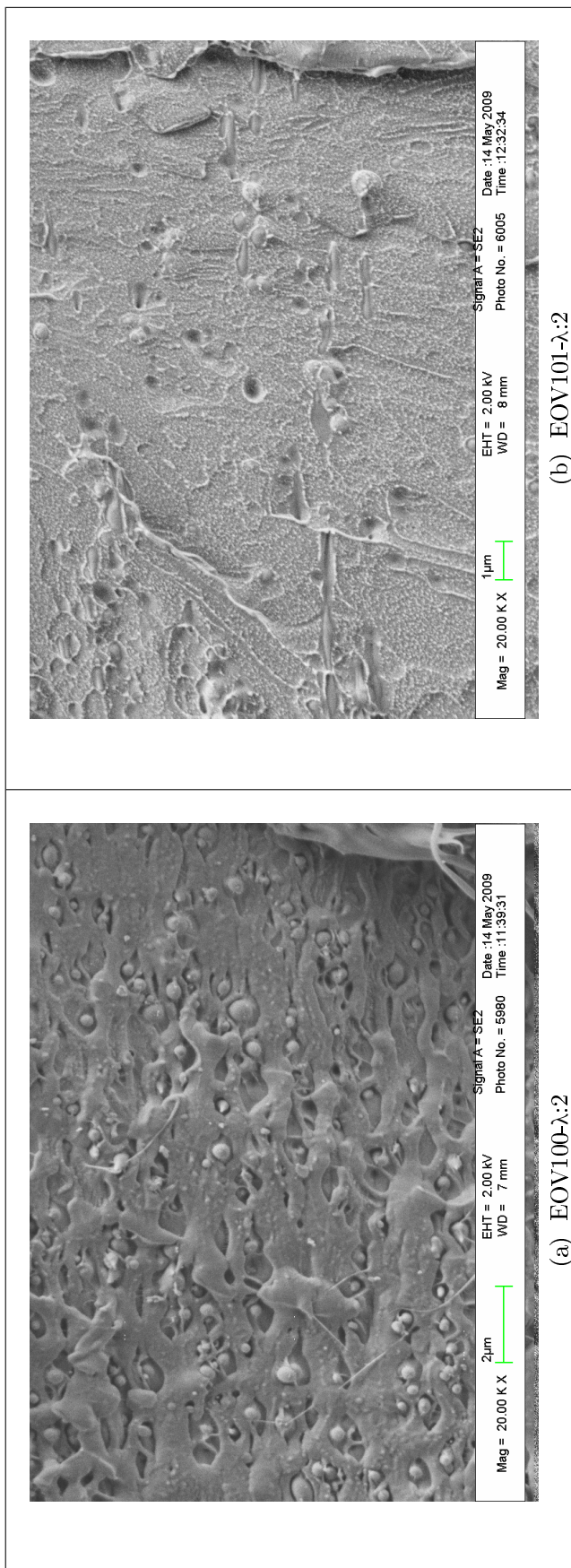


Table 14: SEM images of stretched ($\lambda:2$) PETI blends



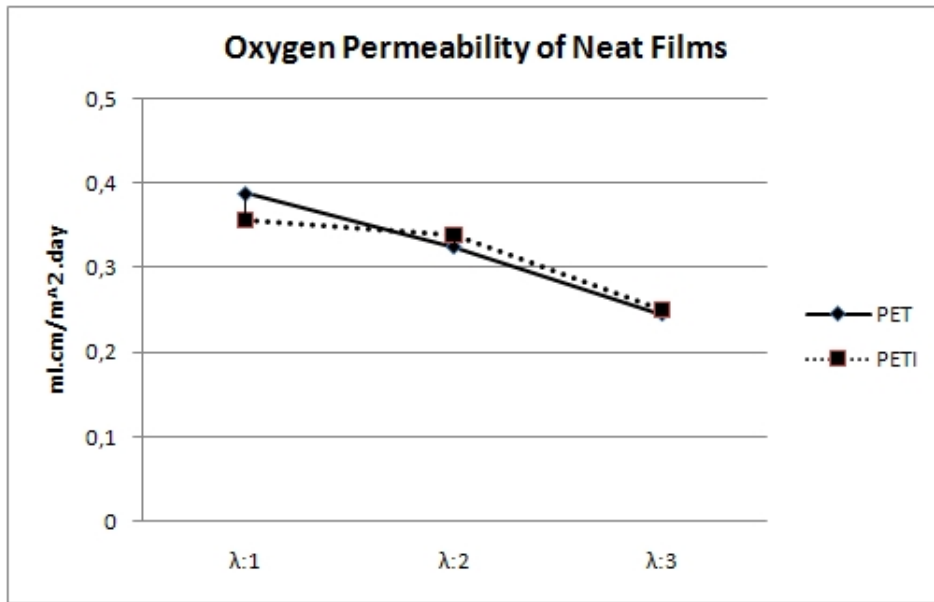


Figure 13: Comparison of oxygen permeability values of neat PET and PETI films

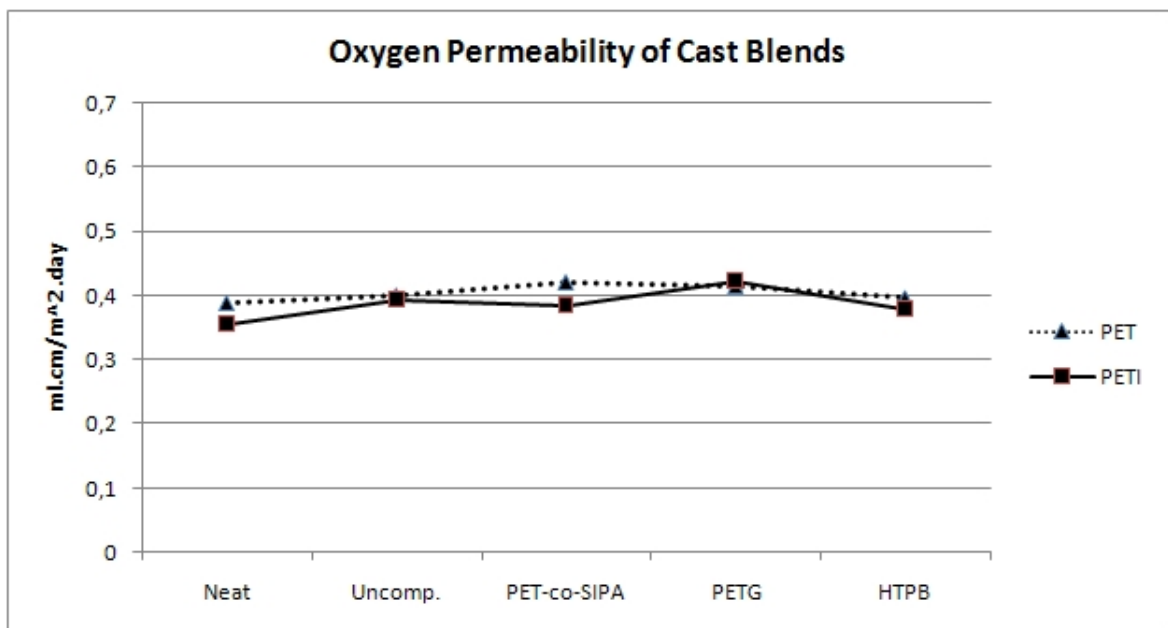


Figure 14: Comparison of oxygen permeability values of cast PET and PETI blends

The unoriented neat PETI has a slightly lower OP value than that of the un-oriented neat PET with 0.356 ml.cm/m².day. Orientation results in lowering the oxygen gas permeability of the neat PETI as in the case of the neat PET film (0.339 for λ:2 and 0.250 for λ:3). Introduction of EVOH to the neat PETI without a compatibilizer increases the OP values (cast EO100: 0.394). Addition of

PET-co-SIPA (EOV101) and HTPB (EOV103) as compatibilizers to the cast PETI decreased the OP values compared to the uncompatibilized blend, however the values are still higher than the neat PETI (cast - EOV101: 0.386, EOV103: 0.380). When PETG is introduced as compatibilizer (EOV102) the OP increases (cast - EOV102: 0.423). 2 times stretching ($\lambda:2$) improves the oxygen barrier properties of the films by decreasing the OP values ($\lambda:2$ - blend without a compatibilizer EOV100: 0.363, PET-co-SIPA blend EOV101: 0.223, PETG blend EOV102: 0.323, HTPB blend EOV103: 0.103). 3 times stretching ($\lambda:3$), decreased the OP values of uncompatibilized blend (EOV100: 0.356) and PET-co-SIPA containing blend (EOV101: 0.134), whereas at the same time, increased the OP values of PETG containing blend (EOV102: 0.369) and HTPB containing blend (EOV013: 0.331), compared to 2 times stretched blends. The lowest OP value was found in 2 times stretched ($\lambda:2$) HTPB containing blend with 0.103 ml.cm/ m^2 .day.

Crystallinity also influences the oxygen gas permeability. As the PET film is extended, PET chains start to align and after a specific stretching ratio has been exceeded strain-induced crystallization occurs [62]. Oxygen permeability is influenced by the crystallinity of polymer because the diffusion of oxygen is affected by more tortuous path through polymer due to increased crystallinity, so that stretching causes the decrease of oxygen permeability [63, 64]. Incorporation of additives may also play a role in crystallinity development through their influence on crystallization (thermal or stress induced or both).

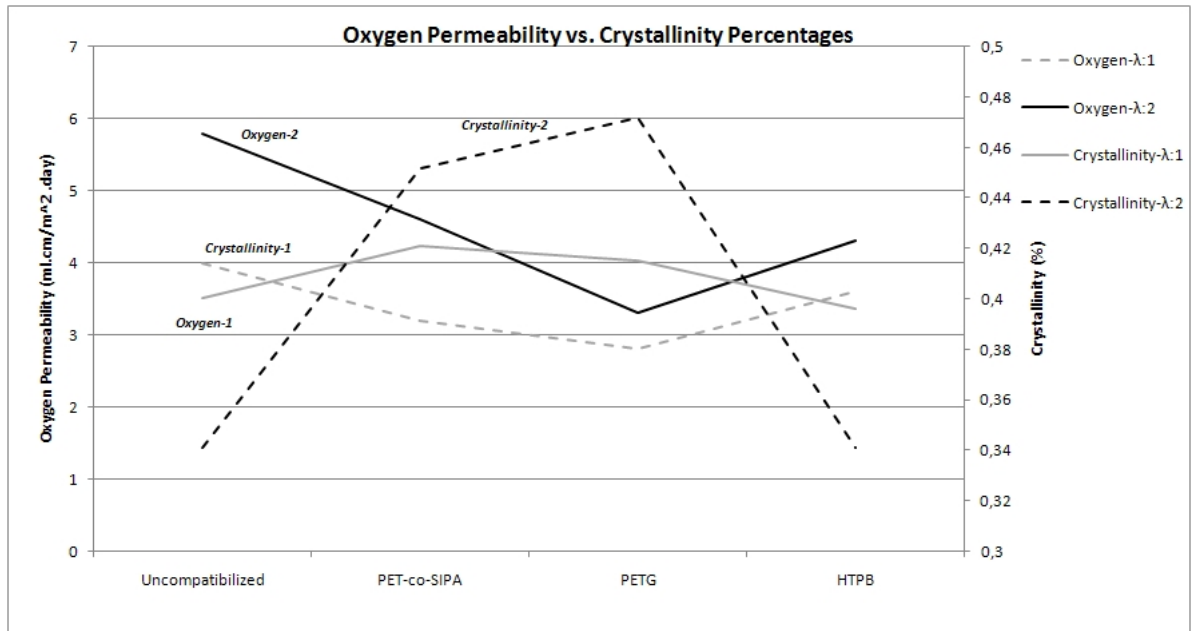


Figure 15: Correlation of oxygen permeability and crystallinity percentage in cast and 2 times stretched PET blends

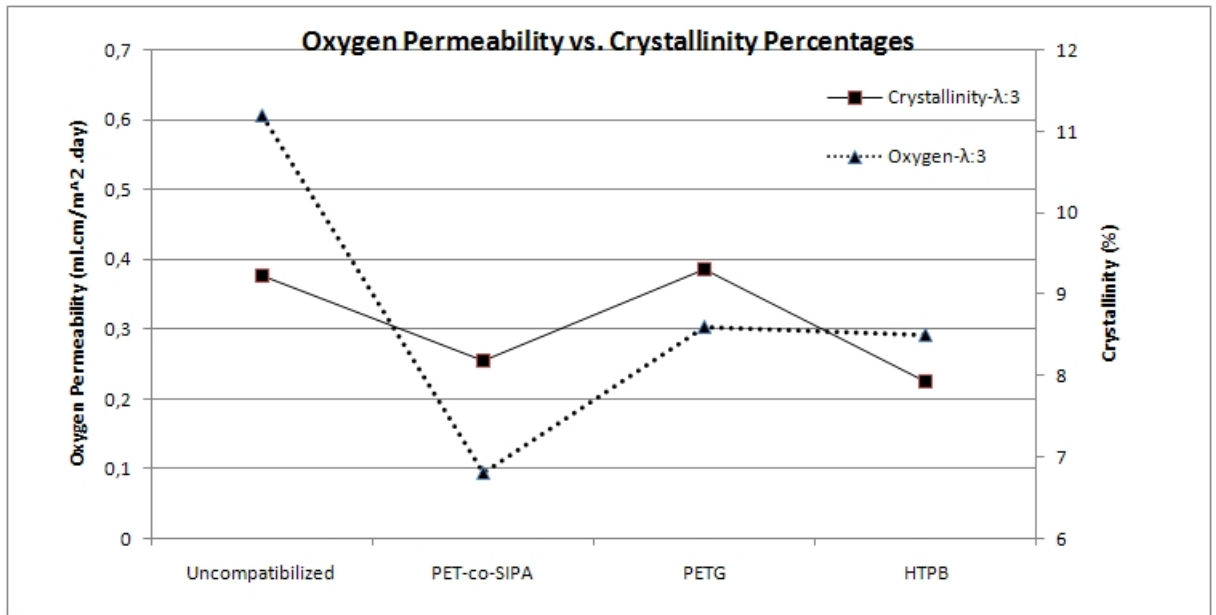


Figure 16: Comparison of oxygen permeability and crystallinity percentage in 3 times stretched PET blends

Correlation of crystallinity values with oxygen permeability values, do not yield a healthy result. As can be seen in Figure 15, the crystallinity percentages and oxygen permeability values in cast and 2 times stretched PET blends ($\lambda:2$), yield an inverse relationship, the exact of what has been expected. Therefore, the change in oxygen permeability values in cast and 2 times stretched PET blends can be explained by the crystallinity percentages. However, in 3 times stretched films ($\lambda:3$), the crystallinity percentage of the samples are in direct relation with the oxygen permeability values as can be seen in Figure 16, contrary to what has been expected. This uncorrelation of oxygen permeability and crystallinity percentage values might be the result of formation of crack and microvoids in the 3 times stretched films increasing permeability of the films, and thus overwriting the correlation of crystallinity percentage and permeability. Such a correlation cannot be made in PETI blends, the crystallinity percentages and oxygen permeability values seem to have no relationship.

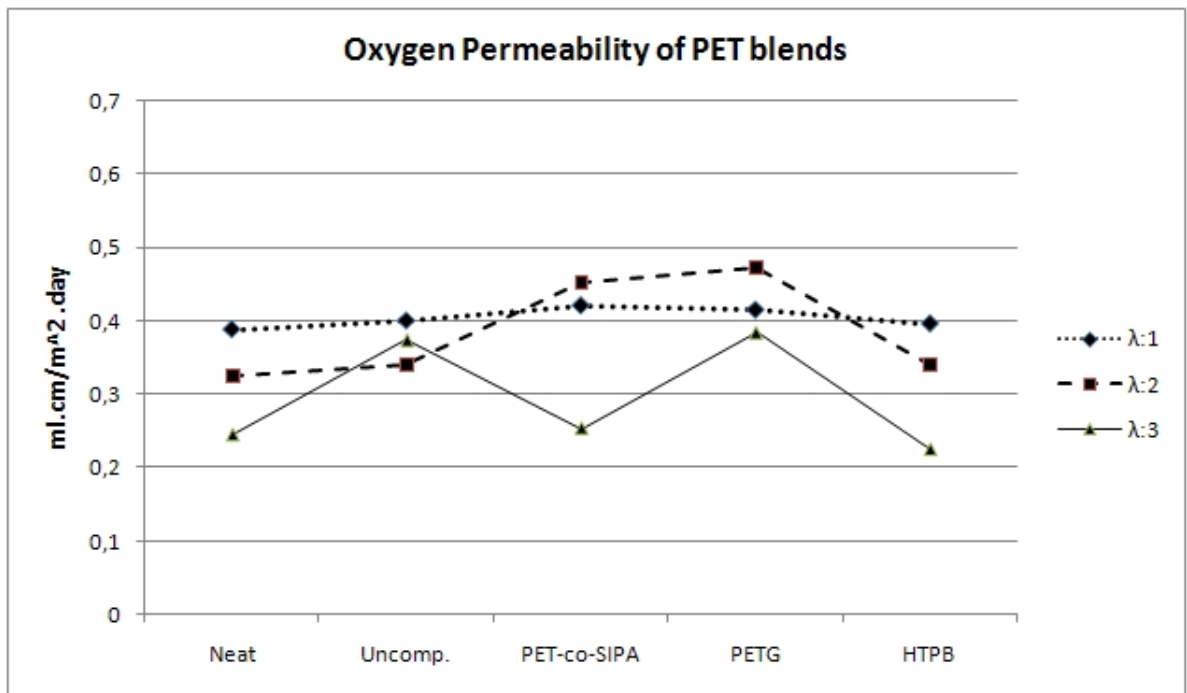


Figure 17: Comparison of oxygen permeability values of cast and stretched PET Blends

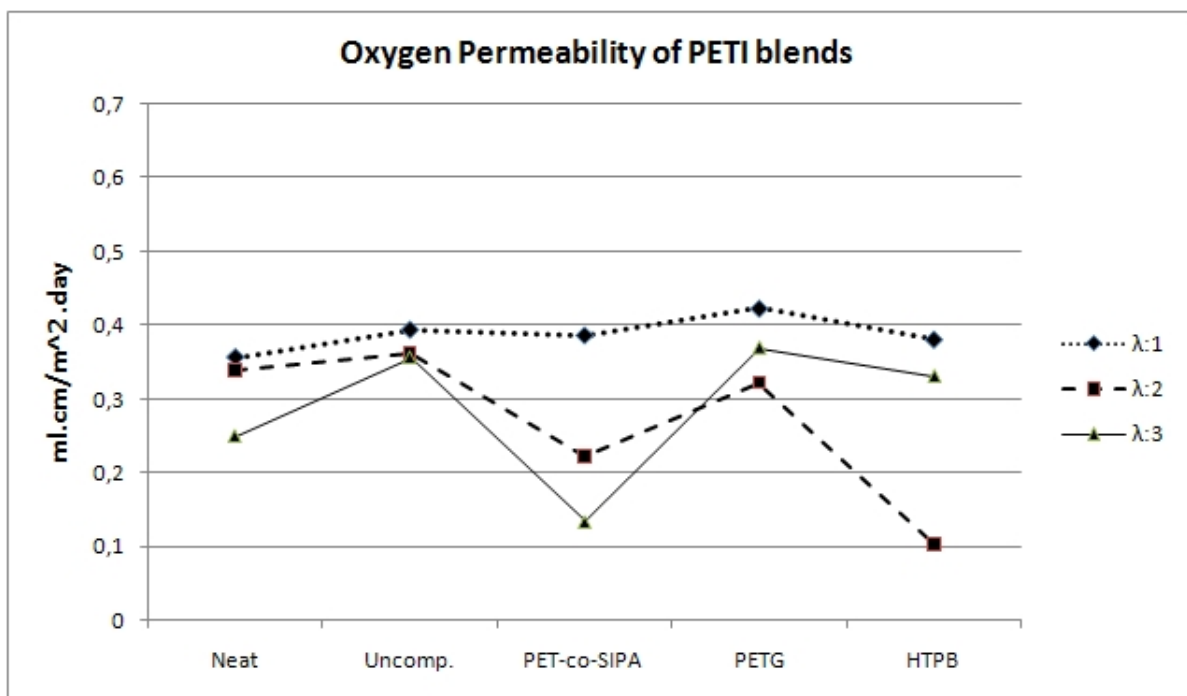


Figure 18: Comparison of oxygen permeability values of cast and stretched PETI Blends

In general, the samples with PETI matrix show slightly better oxygen permeability results than do the samples including the PET matrix. Also, the best results

are obtained using the PETI matrix. In most cases, permeability decreases with increasing stretch ratio. Though, there are exceptions to this statement.

Table 15: Oxygen permeability values of cast and stretched films

Sample	Oxygen Gas Permeability (ml.cm/ m^2 .day)		
	Cast Film	$\lambda:2$	$\lambda:3$
Neat PET	0.388	0.325	0.245
EPV100	0.400	0.341	0.375
EPV101	0.421	0.452	0.254
EPV102	0.415	0.472	0.385
EPV103	0.396	0.341	0.225
Neat PETI	0.356	0.339	0.250
EOV100	0.394	0.363	0.356
EOV101	0.386	0.223	0.134
EOV102	0.423	0.323	0.369
EOV103	0.380	0.103	0.331

13 Water Vapor Permeability

The water vapor permeability (WVP) results of the both the unoriented and stretched films can be seen in Table 13. The WVP value of the unoriented neat PET film reduces from 0.252 g.cm/ m^2 .day to 0.106 ($\lambda:2$) and further down to 0.078 ($\lambda:3$). Addition of EVOH to the cast films without employing compatibilizer decreases the WVP value (cast EPV100: 0.220), furthermore, incorporation of the compatibilizer decreases the WVP values, (PET-co-SIPA containing EPV101: 0.203, PETG containing EPV102 0.120 and HTPB containing EPV103 0.117). 2 times stretching ($\lambda:2$) reduces the WVP values of blends except the PETG containing EPV102 (0.127) ($\lambda:2$ - EPV100: 0.101, EPV101: 0.098, EPV103: 0.106). 3 times stretching ($\lambda:3$) further improves the water vapor barrier property of both the compatibilized and uncompatibilized blends ($\lambda:3$ - EPV100: 0.071, EPV101: 0.081, EPV102: 0.085, EPV103: 0.081). The lowest WVP value has been attained in 3 times stretched uncompatibilized blend (EPV100: 0.071 ($\lambda:3$)).

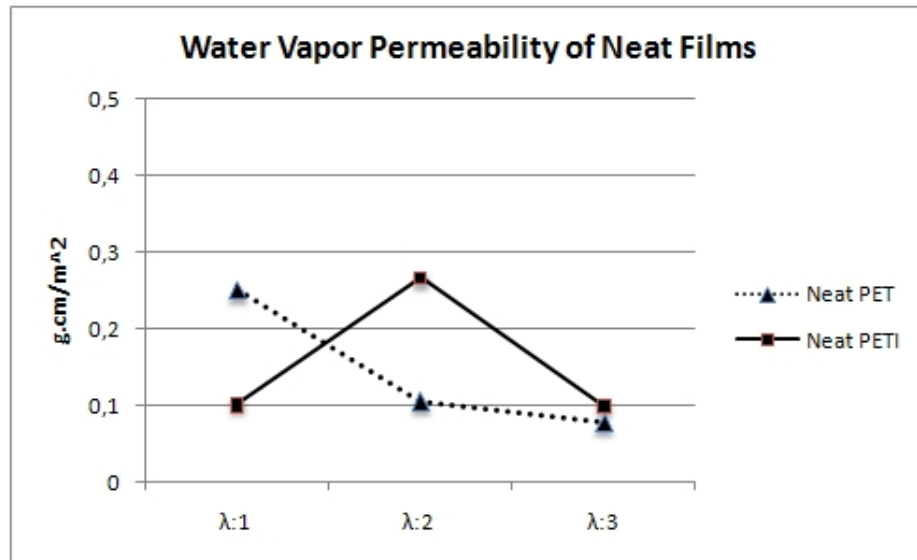


Figure 19: Comparison of water vapor permeability values of neat PET and PETI

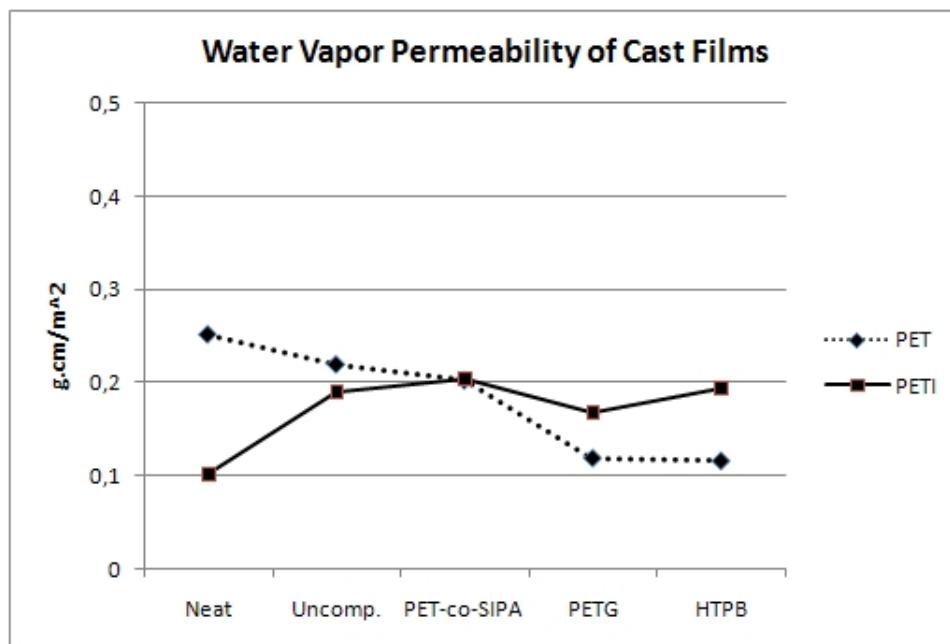


Figure 20: Comparison of cast PETI and PETI Blends

The unoriented neat PETI has lower WVP value than that of the unoriented neat PET with 0.102 g.cm/m².day. Stretching 2 times increased the WVP of the neat PETI unlike the neat PET film, however 3 times stretching lowered the WVP value (0.267 for λ:2 and 0.099 for λ:3). EVOH addition to the neat PETI with or without using a compatibilizer increased the WVP value unlike the behavior in PET blends

(cast - EO100: 0.190, EO101: 0.204, EO102: 0.168, EO103: 0.194). 2 times stretching ($\lambda:2$) improves the oxygen barrier properties of the films by decreasing the WVP values except in the case of HTPB containing blend ($\lambda:2$ - EO103: 0.227), ($\lambda:2$ - blend without a compatibilizer EO100: 0.110, PET-co-SIPA blend EO101: 0.131, PETG blend EO102: 0.104). 3 times stretching ($\lambda:3$), further decreased the WVP values of both the uncompatibilized ($\lambda:3$ - EO100: 0.086) and compatibilized blends ($\lambda:3$ - PET-co-SIPA containing EO101: 0.121, PETG containing EO102: 0.092, HTPB containing EO103: 0.102). The lowest WVP value was found in 3 times stretched ($\lambda:3$) uncompatibilized blend (EO100) with 0.086 g.cm/m².day.

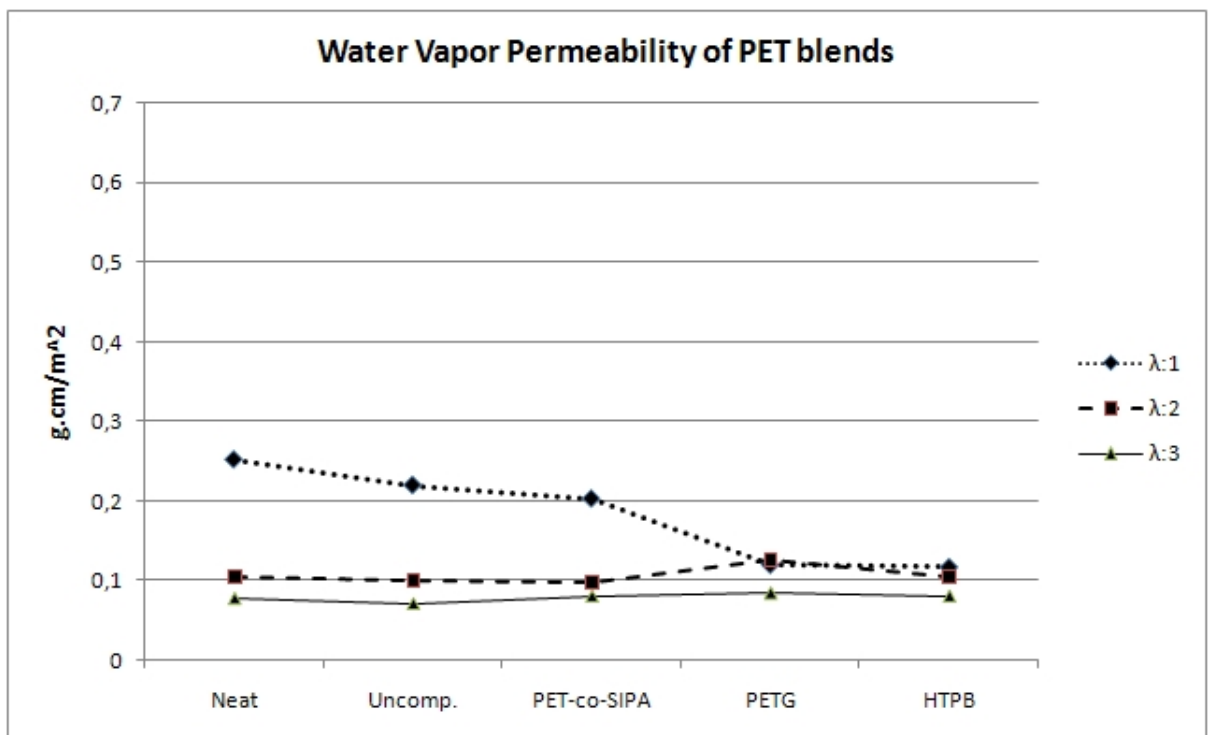


Figure 21: Comparison of water vapor permeability values of cast and stretched PET blends

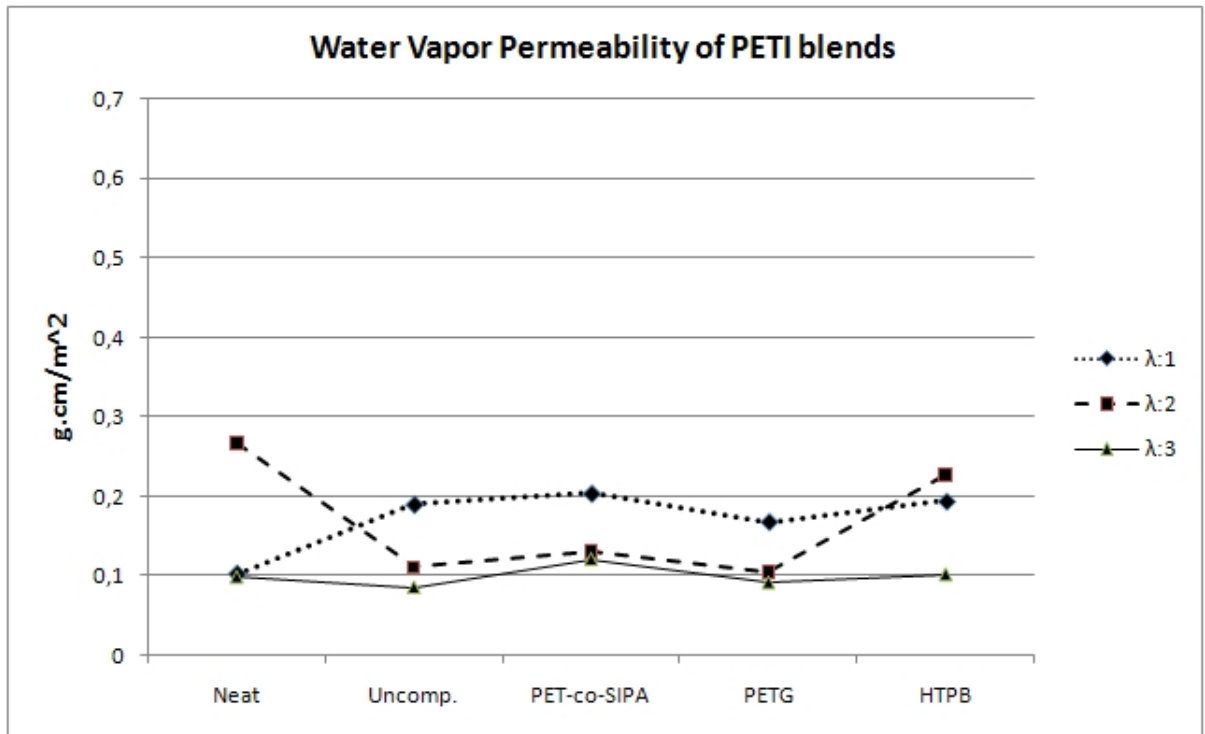


Figure 22: Comparison of water vapor permeability values of cast and stretched PETI blends

Although EVOH is prone to polar molecules such as water, the low amount of EVOH did not yield a sufficient degradation in the water vapor permeability, on the contrary an improvement in this property can easily be seen especially in PET blends. A similar improvement in water vapor permeability was seen in the literature. As the amount of EVOH on the surface is much lower than the amount inside the sample due to surface-volume ratio of the films, the negative effect of the EVOH is eliminated; the effect of the deformed dispersed phase is much greater and thus such an improvement is observed [!!].

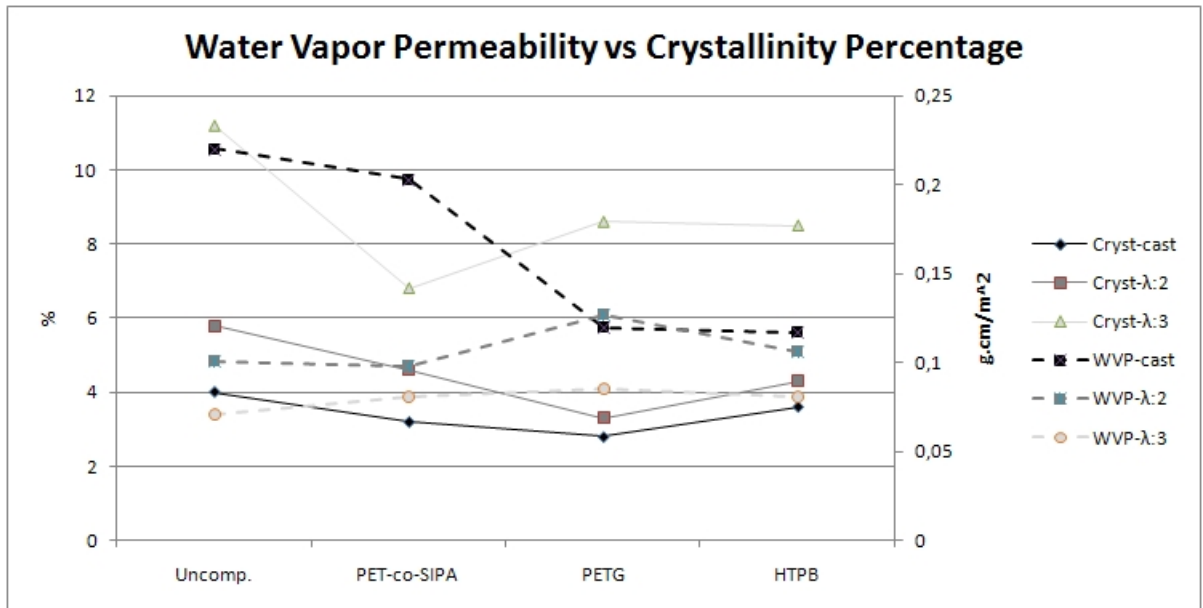


Figure 23: Correlation of water vapor permeability and crystallinity percentages in PET blends

Figure 23 shows the correlation between water vapor permeability values and crystallinity percentages in PET blends. The expected inverse correlation can be detected only in 2 times stretched samples. Whereas in the other samples there cannot be seen a correlation, the two characterization data seems to be random and unrelated. The behavior in water vapor permeability cannot be explained with crystallinity percentages. The other factors affecting permeability such as polymer chemistry, affinity between permeant molecule and polymer film are thought to have more effect on water vapor permeability results than crystallinity percentages.

As permeability is defined to be a function of solubility and diffusivity, solubility parameters for polymeric substances is similar and solubility happens fast. Therefore, diffusivity is the rate-determining step in permeability. The distribution of EVOH throughout the matrix is more or less homogenous, thus by comparing the amount of volume to the amount of surface area, there should be a limited number of EVOH particles on the surface of the film. Therefore, the amount of absorbed penetrant molecules is similar in EVOH added samples. During the diffusion process, thus, approximately the same number of particles are diffused through the film. It is thought that, the vinyl alcohol units of EVOH, form hydrogen bonds with the water molecules. This hydrogen bond formation holds some of the water molecules and obstruct the pathway of the ones that follow. However, as the same bond formation does not take place for non-polar penetrant molecules, the same trend cannot be seen in oxygen permeability. Moreover, if the amount of EVOH in the films were higher than 5 wt %, an increase in water vapor permeability would

be expected. That is, the bond formation between vinyl alcohol units and water molecules and subsequent path obstruction for diffusing water molecules, happens because of the low amount of EVOH. At high amount of EVOH, the vinyl alcohol units are expected to be dissolved in water molecules, leading to plasticization of the blend films, thus degrading the barrier properties.

Table 16: Water vapor permeability values of samples

Sample	Water Vapor Permeability (g.cm/m ² .day)		
	Cast Film	λ :2	λ :3
Neat PET	0.252	0.106	0.078
EPV100	0.220	0.101	0.071
EPV101	0.203	0.098	0.081
EPV102	0.120	0.127	0.085
EPV103	0.117	0.106	0.081
Neat PETI	0.102	0.267	0.099
EOV100	0.190	0.110	0.086
EOV101	0.204	0.131	0.121
EOV102	0.168	0.104	0.092
EOV103	0.194	0.227	0.102

14 Further Notes

Although there has not been a measurement of gloss values of the films, gloss is an important factor if the films are expected to be used in industrial applications for replacement of commercially available plastic packages. The EVOH added films show increased haziness, their transparency is very low. The films tend to have a yellowish coloring. The thickness of the films was not homogenous. Therefore, the possibility of formation of microtears and microvoids after further stretching is increased due to the inhomogeneity of the thickness. The cast films had partial agglomerates scattered throughout the film.

Part IV

Conclusion

All compatibilizers reduced the particle size when compared to those of the uncompatibilized PET/EVOH and PETI/EVOH blends. PETI blends had lower crystallinity percentages compared to those of the PET blends, this is expected because of the *meta* linkages of poly(ethylene isophthalate) hindering the regular ordering of the chains due to the bulky substituent, the aromatic group. Addition of the EVOH decreased the crystallinity of the films. The decrease in crystallinity is due to the vinyl alcohol region of EVOH, hindering the regular structure of the PET matrix, therefore increasing the amorphous percentage in the material. The orientation of the blend films up to 3 times stretching ($\lambda:3$) led to increase in the crystallization due to the strain-induced crystallization occurring by transformation of *gauche* conformers to *trans* conformers and thus leading to nucleation of crystals.

Generally, water vapor barrier properties were improved by introduction of EVOH and further by stretching up to 3 times ($\lambda:3$). The stretched films that have degraded barrier properties are thought to contain microtears and microvoids. There has been a decrease in oxygen barrier properties with the addition of EVOH. This decrease can be explained by the decrease in crystallinity with EVOH addition.

The lowest particle size has been achieved using HTPB (EPV103) and PETG (EPV102). Therefore, in these samples the compatibility of dispersed phase, EVOH and matrix polymer, PET, has been increased. If this study were to be resumed, more focus should be done on the blends with compatibilizers HTPB and PETG with better processing conditions.

Finally, the characterization data delivered incoherent results. Therefore the correlation between permeability values, crystallinity percentages and transition temperatures is very low.

Part V

Future Work

The characterization delivered incoherent results. Therefore expected correlation between different factors affecting were not achieved. The discrepancy in the data is thought to stem from processing. Therefore, the processing conditions should be optimized. The permeability of the films should not be on the orders of magnitude higher than their commercially available counterparts. In other words, the methodology of the study should be optimized. Firstly, it is important that the neat cast polymer films have similar properties to their commercially available counterparts. The compatibilizer addition and stretching should be done after achieving such a polymer film.

The measurement of mechanical properties of the films should be performed and investigated if the mechanical properties of the films are high enough for industrial applications. The gloss values of the films should also be checked for the same reasons. The optical properties of the films can also be checked, with investigation of the birefringence property. The stress and strain values during orientation can be recorded and used for further investigation of crystallinity changes during orientation. During the extrusion process, melt temperatures were not measured. Although the extruder was not of industrial scale, in industrial extruders, melt temperatures and barrel temperatures have differences. These differences might also have impact on the final properties of the polymer blends. Therefore, rather than determination of barrel temperatures, melt temperatures should also be checked. Finally, intrinsic viscosity of the blends should also be checked to see if the PET is degraded or not. The degradation is an essential factor in processing, because if the PET is degraded, then the improvement of barrier properties of cast films is not possible.

The statistical significance of the results should be checked. The characterization data should be repeated at least 3 times to see if the data at hand is coherent. The standard deviation of the data could be helpful in determining this coherence. However, there was not enough time or material for such a large scale study. Therefore, to study the statistical significance of the characterization data, either the time scale of the study could be increased or the scale of the study could be decreased such that the effect of fewer factors could be investigated.

APPENDIX

A Mass Transfer in Polymeric Materials [1]

Diffusion coefficient, D , is a kinetic property. It describes the movement of permeant molecules through the polymeric material. Considering in 1-D, Fick's first law states that:

$$F = -D \frac{\partial c}{\partial x}$$

The solubility coefficient, S , refers to the solvation of permeant molecule in polymer. According to Henry's law, the solubility coefficient is defined in relation to concentration of the penetrant molecule in the polymer film, c , and its pressure, p .

$$S = \frac{c}{p}$$

P , the permeability coefficient, can be derived when Henry's law is applied to Fick's law.

$$F = \frac{q}{At} = -D \frac{\partial c}{\partial x} = -D \frac{c_2 - c_1}{l} = DS \frac{p_2 - p_1}{l} = DS \frac{\nabla p}{l}$$

$$P = DS = \frac{ql}{At \nabla p}$$

where F refers to the flux of the permeant molecules; q , the heat quantity; A , the cross-sectional area of the polymeric material; t , the time; c , the concentration; x , mass transport direction; p , the pressure of the permeant molecules and l , the thickness of the polymer.

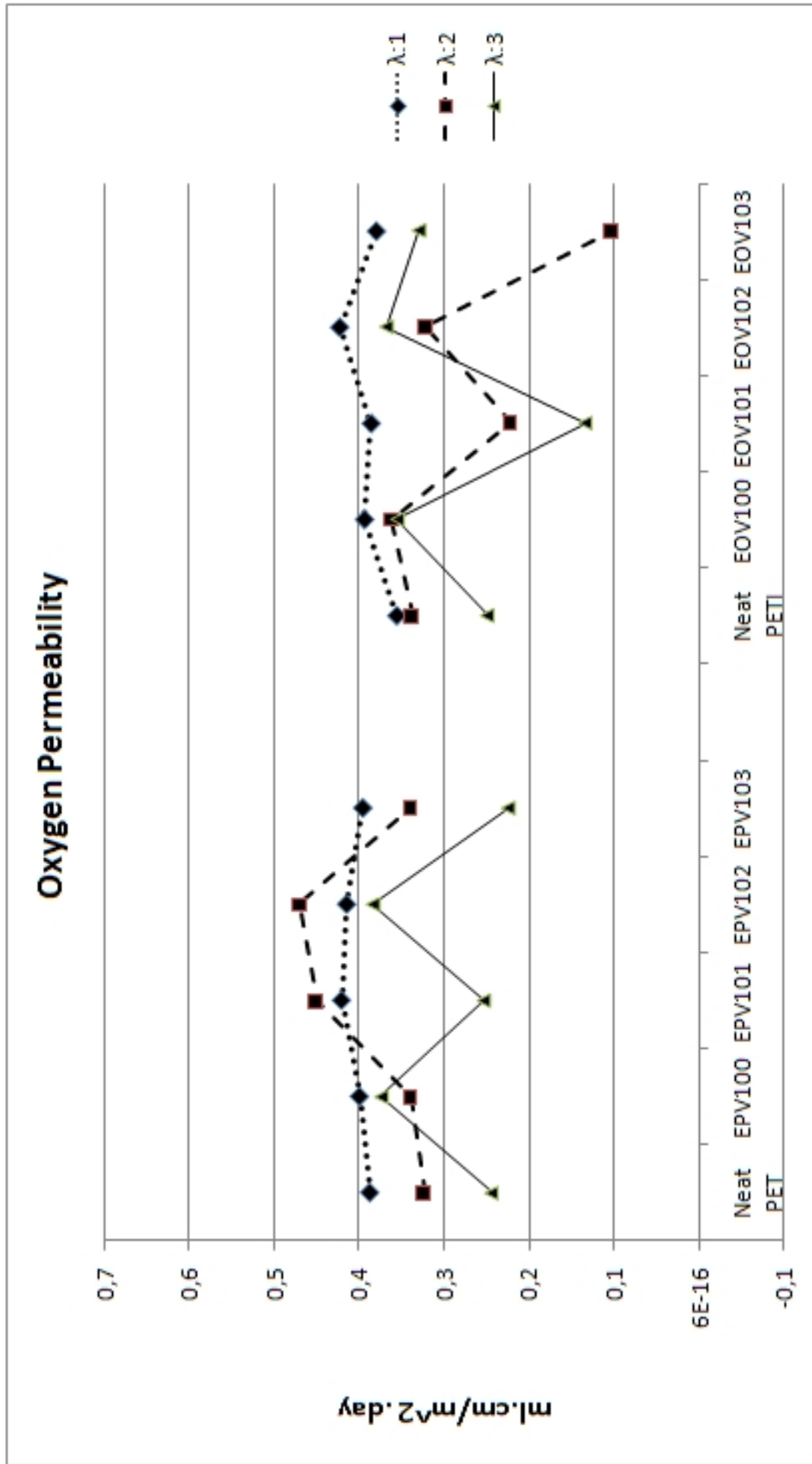


Figure 24: Comparison of oxygen permeability values of all sample films

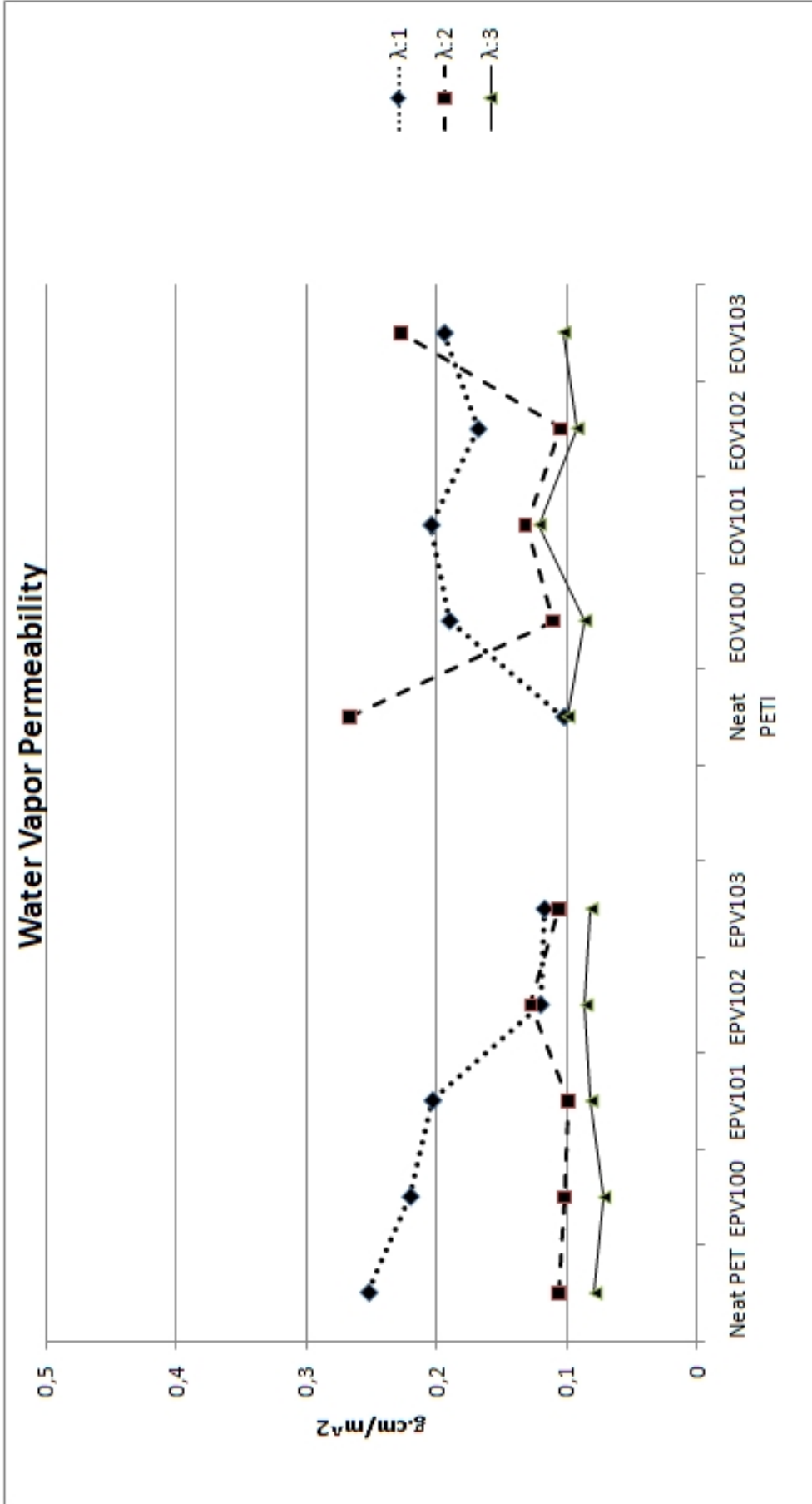


Figure 25: Comparison of water vapor permeability values of all sample films

	Oxygen Permeability (ml.cm/m ² .day)			Water Vapor Permeability (g.cm/m ²)			Crystallinity (%)			
	cast	λ:2	λ:3	cast	λ:2	λ:3	cast	λ:2	λ:3	
<u>PET</u>	Neat	0.388	0.325	0.245	0.252	0.106	0.078	11.0	17.4	28.7
	Uncompatibilized	0.400	0.341	0.375	0.220	0.101	0.071	4.0	5.8	11.2
	PET-co-SIPA	0.421	0.452	0.254	0.203	0.098	0.081	3.2	4.6	6.8
	PETG	0.415	0.472	0.385	0.120	0.127	0.085	2.8	3.3	8.6
HTPB	0.396	0.341	0.225	0.117	0.106	0.081	3.6	4.3	8.5	
<u>PETI</u>	Neat	0.356	0.339	0.250	0.102	0.267	0.099	4.2	8.6	13.3
	Uncompatibilized	0.394	0.363	0.356	0.190	0.110	0.086	0.0	0.9	14.0
	PET-co-SIPA	0.386	0.223	0.134	0.204	0.131	0.121	1.0	1.3	1.6
	PETG	0.423	0.323	0.369	0.168	0.104	0.092	0.0	0.7	0.8
	HTPB	0.380	0.103	0.331	0.194	0.227	0.102	0.0	9.4	4.6

Figure 26: Permeability and crystallinity percentages values of films

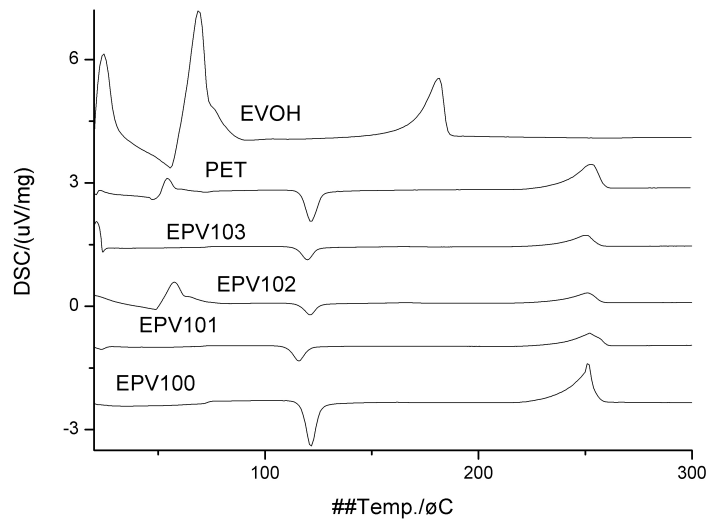


Figure 27: DSC thermograms of cast PET blends

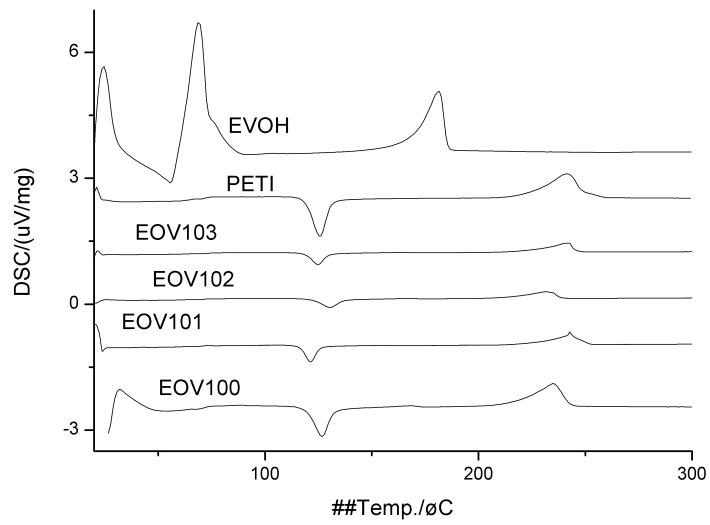


Figure 28: DSC thermograms of cast PETI blends

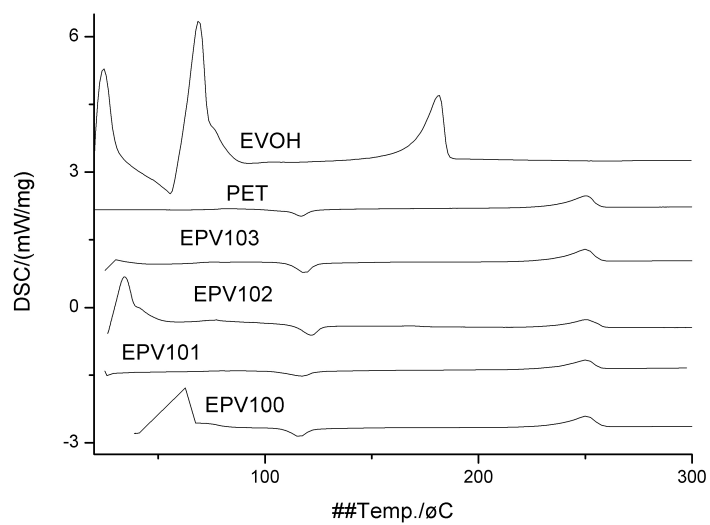


Figure 29: DSC thermograms of 2 times stretched PET blends

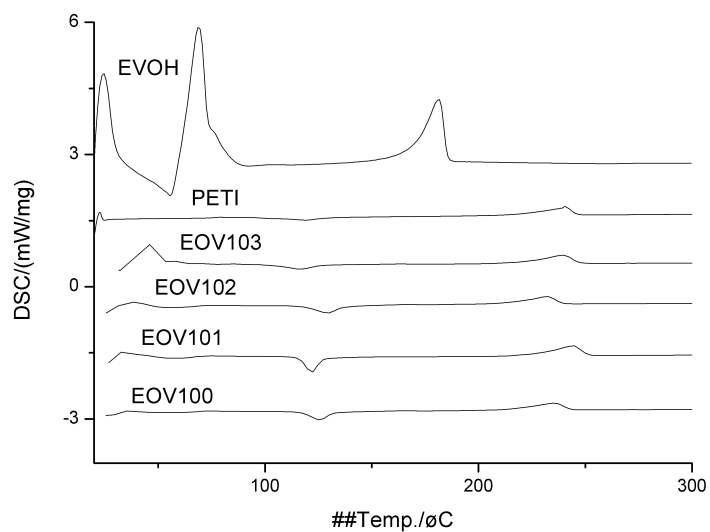


Figure 30: DSC thermograms of 2 times stretched PETI blends

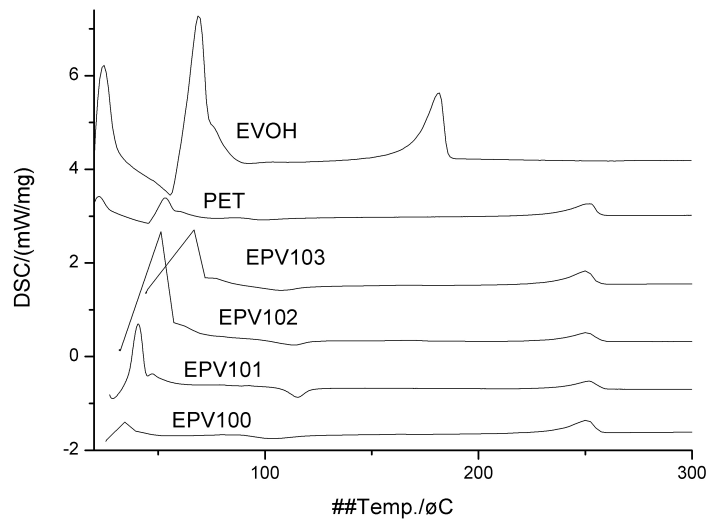


Figure 31: DSC thermograms of 3 times stretched PET blends

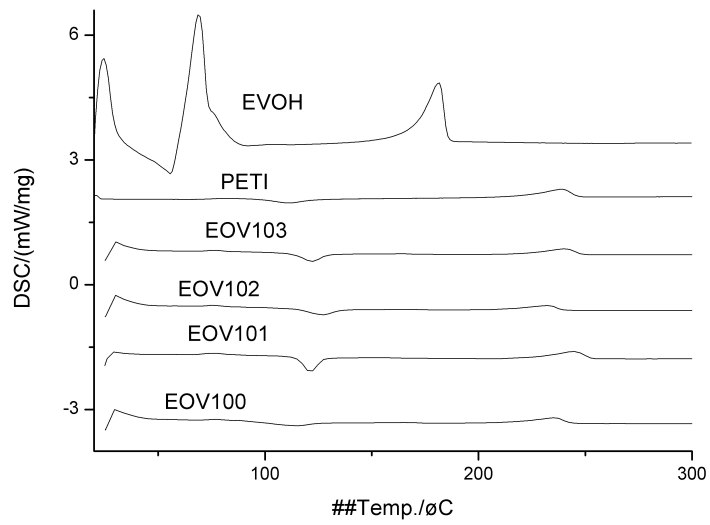


Figure 32: DSC thermograms of 3 times stretched PETI blends

References

- [1] M. Jakobsen and J. Risbo. A simple model for the interaction between water vapour and oxygen transmission in multilayer barrier materials intended for food packaging applications. *Packaging Technology and Science*, 21(4), 2008.
- [2] K.J. Valentas, E. Rotstein, and R.P. Singh. *Handbook of food engineering practice*. CRC Press, 1997.
- [3] Ltd. Labthink Instruments Co. Two different test methods: Differential-pressure method and equal-pressure method, 2009.
- [4] M.B. Huglin and M.B. Zakaria. Comments on expressing the permeability of polymers to gases. *Angewandte Makromolekulare Chemie*, 117(1), 1983.
- [5] S.E.M. Selke. *Understanding plastics packaging technology*. Hanser Gardner Pubns, 1997.
- [6] R.J. Hernandez, S.E.M. Selke, and J.D. Culter. *Plastics packaging: properties, processing, applications, and regulations*. Hanser Munich, 2000.
- [7] Datamonitor. Containers and packaging: Global industry guide, February 2009.
- [8] Piper Jaffray Middle Market Mergers and Acquisitions Group. Packaging industry overview and mergers and acquisitions, ma insights report, February 2009.
- [9] R.H.D. Beswick and DJ Dunn. *Plastics in Packaging: Western Europe and North America*. Rapra Technology, 2002.
- [10] I.A. Taub and R.P. Singh. *Food storage stability*. CRC, 1998.
- [11] AH Varnam and JM Sutherland. *Beverages: technology, chemistry and microbiology*. Aspen Publishers, 1994.
- [12] M. Mathlouthi. *Food packaging and preservation*. Aspen Publishers, 1999.
- [13] R. LEAVERSUCH. Barrier PET bottles. *Plastics technology*, 49(3):48–53, 2003.
- [14] Y.H. Hui. *Handbook of food science, technology, and engineering*. Taylor & Francis, 2006.
- [15] W.A. Hardwick. *Handbook of brewing*. Marcel Dekker, 1995.
- [16] CMD Man and A.A. Jones. *Shelf-life evaluation of foods*. Aspen Pub, 2000.

- [17] J.C. Salamone. *Concise polymeric materials encyclopedia*. CRC press Boca Raton (Fla), 1999.
- [18] G. Bozoklu. *Improvement in Barrier Properties of Polymers Used in Packaging Industry - PET/N-MXD6 Blends*. PhD thesis, 2008.
- [19] N. Qureshi, EV Stepanov, D. Schiraldi, A. Hiltner, and E. Baer. Oxygen-barrier properties of oriented and heat-set poly (ethylene terephthalate). *Journal of Polymer Science Part B: Polymer Physics*, 38(13):1679–1686, 2000.
- [20] Z. Ke and B. Yongping. Improve the gas barrier property of PET film with montmorillonite by in situ interlayer polymerization. *Materials Letters*, 59(27):3348–3351, 2005.
- [21] N. Boutroy, Y. Pernel, JM Rius, F. Auger, H.J. Bardeleben, JL Cantin, F. Abel, A. Zeinert, C. Casiraghi, AC Ferrari, et al. Hydrogenated amorphous carbon film coating of PET bottles for gas diffusion barriers. *Diamond & Related Materials*, 15(4-8):921–927, 2006.
- [22] YS Hu, V. Prattipati, S. Mehta, DA Schiraldi, A. Hiltner, and E. Baer. Improving gas barrier of PET by blending with aromatic polyamides. *Polymer*, 46(8):2685–2698, 2005.
- [23] Y. Yampolskii, I. Pinnau, and B.D. Freeman. *Materials science of membranes for gas and vapor separation*. Wiley Chichester, 2006.
- [24] L.K. Massey. *Permeability properties of plastics and elastomers: A guide to packaging and barrier materials*. Plastics Design Library, 2003.
- [25] J. Comyn. *Polymer permeability*. Chapman & Hall, 1994.
- [26] R. Brown. *Handbook of polymer testing: physical methods*. CRC Press, 1999.
- [27] JM Lagaron, E. Gimenez, R. Gavara, and JJ Saura. Study of the influence of water sorption in pure components and binary blends of high barrier ethylene–vinyl alcohol copolymer and amorphous polyamide and nylon-containing ionomer. *Polymer*, 42(23):9531–9540, 2001.
- [28] IA Nnanna, W. Wu, and YH Hui. *Handbook of food products manufacturing*, 2007.
- [29] A. Azapagic, A. Emsley, and I. Hamerton. *Polymers: the environment and sustainable development*. Wiley, 2003.

- [30] C.I. Martins and M. Cakmak. Control the strain-induced crystallization of polyethylene terephthalate by temporally varying deformation rates: A mechano-optical study. *Polymer*, 48(7):2109–2123, 2007.
- [31] G. Aravinthan and DD Kale. Blends of poly (ethylene terephthalate) and poly (butylene terephthalate). *Journal of Applied Polymer Science*, 98(1), 2005.
- [32] CK Samios and NK Kalfoglou. Acrylic-modified polyolefin ionomers as compatibilizers for poly (ethylene-co-vinyl alcohol)/aromatic copolyester blends. *Polymer*, 42(8):3687–3696, 2001.
- [33] JM Lagaron, E. Gimenez, JJ Saura, and R. Gavara. Phase morphology, crystallinity and mechanical properties of binary blends of high barrier ethylene–vinyl alcohol copolymer and amorphous polyamide and a polyamide-containing ionomer. *Polymer*, 42(17):7381–7394, 2001.
- [34] D. Cava, L. Cabedo, E. Gimenez, R. Gavara, and JM Lagaron. The effect of ethylene content on the interaction between ethylene–vinyl alcohol copolymers and water:(I) Application of FT-IR spectroscopy to determine transport properties and interactions in food packaging films. *Polymer Testing*, 25(2):254–261, 2006.
- [35] CK Samios and NK Kalfoglou. Compatibilization of poly (ethylene-co-vinyl alcohol)(EVOH) and EVOH/HDPE blends with ionomers. Structure and properties. *POLYMER-LONDON-*, 39:3863–3870, 1998.
- [36] K.M. Kit, J.M. Schultz, and R.M. Gohil. Morphology and barrier properties of oriented blends of poly (ethylene terephthalate) and poly (ethylene 2, 6-naphthalate) with poly (ethylene-co-vinyl alcohol). *Polymer Engineering & Science*, 35(8), 1995.
- [37] J.H. Yeo, C.H. Lee, C.S. Park, K.J. Lee, J.D. Nam, and S.W. Kim. Rheological, morphological, mechanical, and barrier properties of PP/EVOH blends. *Advances in Polymer Technology*, 20(3):191–201, 2001.
- [38] K. Kimura, T. Katoh, and SP McCarthy. Compatibilization of PET/EVOH Blends by Reactive Extrusion. In *TECHNICAL PAPERS OF THE ANNUAL TECHNICAL CONFERENCE-SOCIETY OF PLASTICS ENGINEERS INCORPORATED*, pages 2626–2631. SOCIETY OF PLASTICS ENGINEERS INC, 1996.
- [39] MM Coleman, X. YANG, H. ZHANG, and PC Painter. Ethylene-co-vinyl alcohol blends. *Journal of macromolecular science. Physics*, 32(3):295–326, 1993.

- [40] Y. Nir, M. Narkis, and A. Siegmund. Partially miscible EVOH/copolyamide-6/6.9 blends: Thermal, dynamic-mechanical and shear rheology behavior. *Polymer Engineering & Science*, 38(11), 1998.
- [41] T.S. Ellis. Reverse exfoliation in a polymer nanocomposite by blending with a miscible polymer. *Polymer*, 44(21):6443–6448, 2003.
- [42] T.M. Wu, C.C. Chang, and T.L. Yu. Crystallization of Poly (ethylene terephthalate-co-isophthalate). *Journal of Polymer Science Part B: Polymer Physics*, 38(19), 2000.
- [43] B. Li, J. Yu, S. Lee, and M. Ree. Poly (ethylene terephthalate co ethylene isophthalate)?relationship between physical properties and chemical structures. *European Polymer Journal*, 35(9):1607–1610, 1999.
- [44] W.J. Walczak and R.P. Wool. Investigation of polymer melt relaxation mechanisms via dynamic infrared dichroism. *Macromolecules*, 24(16):4657–4665, 1991.
- [45] A.K. Oultache, X. Kong, C. Pellerin, J. Brisson, M. Pérolet, and R.E. Prud’homme. Orientation and relaxation of orientation of amorphous poly (ethylene terephthalate). *Polymer*, 42(21):9051–9058, 2001.
- [46] P. Chandran and S. Jabarin. Biaxial orientation of poly (ethylene terephthalate). Part I: Nature of the stress-strain curves. *Advances in Polymer Technology*, 12(2), 1993.
- [47] J. Guevremont, A. Aji, KC Cole, and MM Dumoulin. Orientation and conformation in poly (ethylene terephthalate) with low draw ratios as characterized by specular reflection infra-red spectroscopy. *POLYMER-LONDON-*, 36:3385–3385, 1995.
- [48] A. Aji, J. Guevremont, KC Cole, and MM Dumoulin. Orientation and structure of drawn poly (ethylene terephthalate). *POLYMER-LONDON-*, 37:3707–3714, 1996.
- [49] D. Kawakami, S. Ran, C. Burger, C. Avila-Orta, I. Sics, B. Chu, B.S. Hsiao, T. Kikutani, et al. Superstructure evolution in poly (ethylene terephthalate) during uniaxial deformation above glass transition temperature. *Macromolecules*, 39(8):2909–2920, 2006.
- [50] D. Kawakami, B.S. Hsiao, S. Ran, C. Burger, B. Fu, I. Sics, B. Chu, and T. Kikutani. Structural formation of amorphous poly (ethylene terephthalate)

- during uniaxial deformation above glass temperature. *Polymer*, 45(3):905–918, 2004.
- [51] S. De Petris, P. Laurienzo, M. Malinconico, M. Pracella, and M. Zendron. Study of blends of Nylon 6 with EVOH and carboxyl-modified EVOH and a preliminary approach to films for packaging applications. *Journal of Applied Polymer Science*, 68(4):637–648, 1998.
- [52] DC Bassett. *Principles of polymer morphology*. Cambridge University Press, 1981.
- [53] C.A. Harper. *Handbook of plastics, elastomers, and composites*. McGraw-Hill Professional, 2002.
- [54] B.B. Doudou, E. Dargent, and J. Grenet. Relationship between Draw Ratio and Strain-Induced Crystallinity in Uniaxially Hot-Drawn PET MXD6 Films. *Journal of Plastic Film and Sheeting*, 21(3):233, 2005.
- [55] LA Utracki. *Polymer blends handbook*. Kluwer Academic Publishers, 2002.
- [56] T.D. Patcheak and S.A. Jabarin. Structure and morphology of PET/PEN blends. *Polymer*, 42(21):8975–8985, 2001.
- [57] S. Datta and D.J. Lohse. *Polymeric compatibilizers: uses and benefits in polymer blends*. Hanser New York, 1996.
- [58] M. Fiorini, B. Bracci, F. Pilati, and E. Fabbri. PBT modification with EVA/EVOH copolymers: a morphological study. In *Macromolecular Symposia*, volume 176. WILEY-VCH Verlag GmbH Weinheim, 2001.
- [59] WE Baker, C. Scott, and GH Hu. *Reactive Polymer Blending (Progress in Polymer Processing)*. Hanser Gardner Publications, 2001.
- [60] E. Földes and B. Pukánszky. Miscibility–structure–property correlation in blends of ethylene vinyl alcohol copolymer and polyamide 6/66. *Journal of colloid and interface science*, 283(1):79–86, 2005.
- [61] T.A. Osswald and J.P. Hernández-Ortiz. *Polymer processing: modeling and simulation*. Hanser Gardner Publications, 2006.
- [62] SA Jabarin. A Course on PET Technology. *The University of Toledo, Toledo, OH*, 1997.
- [63] S.A. Jabarin. Orientation studies of poly (ethylene terephthalate). *Polymer Engineering & Science*, 24(5), 1984.

- [64] J. Brace. The Lecture Note of Transport in Plastics. *The University of Toledo, Toledo, OH*, 2006.